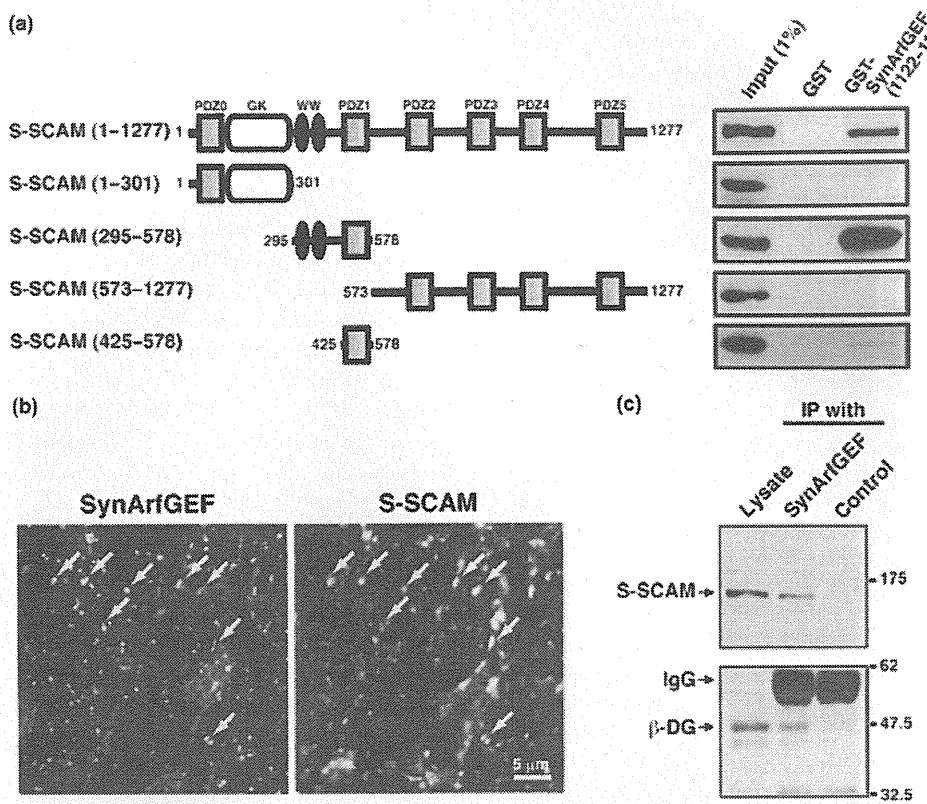

Fig. 9 Interaction of synArfGEF with S-SCAM. (a) Pull down assays. COS-7 cells were transfected with the S-SCAM constructs shown in the left panel and subjected to pull down assays with GST-synArfGEF 1122–1194. Note the interaction of GST-synArfGEF 1122–1194 with S-SCAM fragments 1–1277, 295–578, and 425–578. (b) Immunofluorescent staining of the cerebellar molecular layer, showing the partial colocalization of synArfGEF and S-SCAM (arrows). (c) Co-immunoprecipitation assays. Deoxycholate-solubilized P2 fractions were immunoprecipitated with anti-synArfGEF IgG or normal rabbit IgG and subjected to Western blot analysis with antibodies against S-SCAM and β-dystroglycan (β-DG). Note the co-immunoprecipitation of S-SCAM and β-dystroglycan with synArfGEF from brain lysates.

β-dystroglycan from the deoxycholate-solubilized P2 fraction (Fig. 9c). Taken together, these results suggest that synArfGEF is likely to be present in the DGC and associate with S-SCAM at inhibitory synapses.

Discussion

The BRAG/IQSEC family is composed of three members, IQ-ArfGEF/BRAG1/IQSEC2, GEP100/BRAG2/IQSEC1, and synArfGEF/BRAG3/IQSEC3, all of which share characteristic domain organization containing an N-terminal IQ-like motif, a central Sec7 domain and pleckstrin homology domain (Table 1). GEP100/BRAG2/IQSEC1, a prototypical member of this family, was shown to activate Arf6 *in vitro* and *in vivo* (Someya *et al.* 2001; Morishige *et al.* 2008). IQ-ArfGEF/BRAG1/IQSEC2 was subsequently shown to activate Arf6 using pull down assays with GST-GGA1 (Sakagami *et al.* 2008). In this study, we have shown that synArfGEF/BRAG3/IQSEC3 also functions as a GEF for Arf6 *in vivo* by using pull down and transferrin incorporation assays. However, we were unable to conclusively demonstrate the GEF activity of synArfGEF toward Arf1, because co-transfection of synArfGEF and Arf1 increased total Arf1 in the lysate to the same extent as GTP-Arf1 pulled down by GST-GGA1. By contrast, Hattori *et al.* (2007) have previously shown that KIAA1110, encoding a human homologue of synArfGEF, exhibits GEF activity toward Arf1 but not Arf6 using an Arf pull down assay with the same GST-GGA1. The reasons for this discrepancy are unknown at present. However, as KIAA1110 is a partial 770 amino acid protein corresponding to amino acids 439–1194 of rat synArfGEF, the complete structure of synArfGEF may be required for GEF activity toward Arf6.

The PSD of excitatory synapses is known to contain a diverse array of GEFs and GTPase-activating proteins (GAPs) for small GTPases: Ras-GAP (synGAP) (Chen *et al.* 1998), Arf-GEFs (BRAG1, BRAG2b) (Murphy *et al.* 2006; Dosemeci *et al.* 2007; Sakagami *et al.* 2008), Arf-GAPs (GIT1 and PIKE-L) (Peng *et al.* 2004), Rac-GEF (Kalirin) (Penzes *et al.* 2000), Rap-GEF (cAMP-GEFII/Epac2) (Peng

Table 1 BRAG/IQSEC family proteins and interactors and key roles in synaptic function

Gene symbol and chromosomol location	Other names	GTPase specificity	Interacting proteins/proposed biological function	References
IQSEC1 3p25.2 (human) *Iqsec1* 6qDI (mouse)	GEP 100 BRAG2 IQSEC1 KIAA0763 p100	Arf1, Arf5, **Arf6**	• BRAG2 activating of Arf6 regulates endocytosis and recycling of β1 integrins • Alpha-catenin binding to ArfGEP100 activates Arf6, resulting in E-cadherin recycling and actin re-modelling • BRAG2 interacts with α-amino-3-hydroxy-5-methyl-4-isoxazolepropionate (AMPA) receptor subunit GluA2 and activates Arf6, thereby internalizing synaptic AMPA receptors upon LTD induction	Dunphy *et al.* (2006) Hiroi *et al.* (2006) Scholz *et al.* (2010)
IQSEC2 Xp11.22 (human) *Iqsec2* XqF3 (mouse)	IQ-ArfGEF BRAG1 IQSEC2 K1AA0522	Arf1, **Arf6**	• IQ-ArfGEF selectively activates Arf6 and forms a complex with NDMA receptors via interactions with PSD95 at excitatory synapses • IQ-ArfGEF interacts with insulin receptor tyrosine kinase substrate p53 (IRSp53) at excitatory PSDs via its C-terminal proline-rich sequence • IQ-ArfGEF mRNA is dendritically localized • IQ-ArfGEF/BRAG1 localizes as retinal synaptic ribbons and forms a protein complex with RIBEYE • Missense mutations in *IQSEC2* cause non-syndromic X-linked intellectual disability	Murphy *et al.* (2006) Dosemeci *et al.* (2007) Sanda *et al.* (2009) Katsumata *et al.* (2009) Shoubridge *et al.* (2010)
IQSEC3 l2pl3.33 (human) *Iqsec3* 6qF1 (mouse)	SynArfGEF BRAG3 IQSEC3 KIAA1110	Arf1, **Arf6**	• SynArfGEF is able to interact with PSD-95, SAP97 and Homer/Vesll/PSD-Zip45 via a C-terminal PDZ-binding motif • SynArfGEF mRNA is dendritically localized • SynArfGEF selectively activates Arf6 and interacts with scaffolding proteins utrophin/dystrophin and S-SCAM/MAGI-2 at inhibitory synapses	Inaba *et al.* (2004) Hattori *et al.* (2007) This study

et al. 2004), and Rap-GAP (SPAR) (Pak *et al.* 2001). These regulatory proteins for small GTPases are proposed to modulate synaptic transmission by regulating the formation and maintenance of dendritic spines and synapses through the actin cytoskeleton reorganization (Penzes *et al.* 2001; Zhang *et al.* 2003, 2005; Vazquez *et al.* 2004; Woolfrey *et al.* 2009). Among the BRAG family, IQ-ArfGEF/BRAG1/IQSEC2 was shown to localize at the PSD of excitatory synapses and form a protein complex with NMDA-type glutamate receptors, possibly via an interaction with PSD-95 (Murphy *et al.* 2006; Dosemeci *et al.* 2007; Sakagami *et al.* 2008) and insulin receptor tyrosine kinase substrate of 53 kDa (IRSp53) (Sanda *et al.* 2009) (Table 1). Mutations in *IQSEC2* have recently been reported in patients with non-syndromic X chromosome-linked intellectual disability (Shoubridge *et al.* 2010). Interestingly, mutations in three of four separate families with non-syndromic X chromosome-linked intellectual disability lead to amino acid substitutions in the Sec7 domain and consequent reduction of the GEF activity toward Arf6, suggesting the functional significance of IQSEC2-Arf6 pathway in neuronal morphology or synaptic plasticity (Shoubridge *et al.* 2010). In sharp contrast, we show that synArfGEF localizes preferentially at post-synaptic specializations of inhibitory synapses. This major finding was confirmed by several independent lines of immunohistochemical evidence. To our knowledge, the only known regulator of small GTPases found at inhibitory post-synaptic specializations is collybistin, a GEF for Cdc42, which was identified as an interacting protein for gephyrin by yeast two-hybrid screening (Kins *et al.* 2000). Thus, synArfGEF is listed as the second known regulator of GTPase that shows preferential localization at post-synaptic specializations of inhibitory synapses.

What are the potential roles of synArfGEF at inhibitory synapses? The Arf family comprises six structurally related members that regulate membrane trafficking and the actin cytoskeleton (D'Souza-Schorey and Chavrier 2006). Of the six Arf members, Arf6 is localized at the plasma membrane and endosomes, and regulates the endosome-plasma membrane traffic and remodeling of the actin cytoskeleton at the cell surface. At synapses, the submembrane cytoskeleton is known to regulate the number and dynamics of neurotransmitter receptors on the post-synaptic membrane, thereby modulating synaptic efficacy. At inhibitory synapses, both

actin and microtubules have been shown to regulate the lateral diffusion and stabilization of glycine receptors and gephyrin (Charrier *et al.* 2006). In addition, gephyrin interacts with various regulatory proteins for the cytoskeleton, including polymerized tubulin (Kirsch *et al.* 1991), profilin (Mammoto *et al.* 1998) and mammalian enabled/vasodilator stimulated phosphoprotein (Giesemann *et al.* 2003). In turn, gephyrin depends on both actin and microtubules for synaptic apposition and scaffold formation (Kirsch and Betz 1995). It is therefore possible that synArfGEF may initiate local remodeling of the synaptic submembrane actin cytoskeleton through the activation of Arf6, thereby modulating the lateral diffusion and stabilization of neurotransmitter receptors and gephyrin at inhibitory synapses.

Another noteworthy finding is that synArfGEF interacts with utrophin/dystrophin and S-SCAM via a PY motif and PDZ-binding motif in the C-terminal region, respectively. The ability of synArfGEF to bind utrophin/dystrophin was verified by both yeast two-hybrid and pull down assays. Although we failed to detect dystrophin or utrophin in co-immunoprecipitation assays, β-dystroglycan and S-SCAM were immunoprecipitated from brain lysates by the anti-synArfGEF IgG. Consistent with previous findings demonstrating that dystrophin and S-SCAM are localized to inhibitory synapses (Knuesel *et al.* 1999; Sumita *et al.* 2007), immunostaining showed the colocalization of synArfGEF with dystrophin and S-SCAM. However, the anti-utrophin antibody raised in this study did not result in any immunolabeling in the cultured hippocampal neurons. This is consistent with previous findings suggesting that utrophin transcripts are predominantly expressed in endothelial cells of blood vessels rather than in neurons (Knuesel *et al.* 2000). Hence, it is likely that S-SCAM and dystrophin, but not utrophin, are physiological binding partners for synArfGEF. At inhibitory synapses, dystrophin forms the DGC with α- and β-dystroglycan, syntrophin, and α- and β-dystrobrevin. Intriguingly, S-SCAM was shown to interact directly with two inhibitory post-synaptic components, β-dystroglycan and neuroligin-2 (Sumita *et al.* 2007). Thus, the interaction of synArfGEF with dystrophin and S-SCAM enables synArfGEF to activate Arf6 in the proximity of the DGC and neuroligin-2 at inhibitory post-synaptic specializations. Mdx mice lacking a long form of dystrophin exhibit a marked reduction in the clustering of $GABA_A$Rs containing the α2 subunit but retain gephyrin clustering in the cerebellar cortex, suggesting a dystrophin-dependent and gephyrin-independent mechanism for the clustering of selected $GABA_A$R subtypes. In the future, it will be of particular interest to examine the possibility that synArfGEF is involved in the dystrophin-dependent clustering of $GABA_A$Rs through Arf6-dependent actin cytoskeleton remodeling.

Finally, it should be noted that the interaction of synArfGEF with dystrophin and S-SCAM cannot account for the specific mechanism for the targeting of synArfGEF to inhibitory synapses, because dystrophin and S-SCAM are only present at a subset of inhibitory synapses and S-SCAM is present at both excitatory and inhibitory synapses (Knuesel *et al.* 1999; Levi *et al.* 2002; Sumita *et al.* 2007). Therefore, additional factors are required for specific targeting of synArfGEF to inhibitory synapses.

In conclusion, we have demonstrated that synArfGEF activates Arf6 and localizes preferentially at inhibitory post-synaptic specializations, forming a protein complex with the DGC and S-SCAM using distinct binding motifs. These findings link Arf6 signaling pathways to inhibitory synapses and suggest that synArfGEF may influence dynamic processes affecting the synaptic localization of inhibitory $GABA_A$ and glycine receptors.

Acknowledgements

We thank Dr Kazuhisa Nakayama (Kyoto University Graduate School of Pharmaceutical Sciences) for the expression vectors for HA-tagged Arf1, Arf6 and GST-GGA1-GAT fusion protein, Dr Masanobu Satake (Tohoku University) for FLAG-tagged Arf6 in pCAGGS-neo, Dr James M. Ervasti (University of Minnesota) for FLAG-utrophin in pFASTBac1, Dr Jun-ichi Miyazaki (Osaka University Medical School) for pCAGGS vector. This work was supported by Grants-in-Aid for Scientific Research to H.S. (#2165049 and #22300114) from the Ministry of Education, Science, Sports, Culture, and Technology of Japan and grants from Kitasato University (All Kitasato Project Study and Integrative Research Program #2009-A01).

Supporting information

Additional Supporting information may be found in the online version of this article:

Figure S1. The specificity of antibodies against gephyrin, S-SCAM, and utrophin.

Figure S2. Characterization of anti-synArfGEF antibodies by immunostaining.

Table S1. Primer combinations used in this study.

As a service to our authors and readers, this journal provides supporting information supplied by the authors. Such materials are peer-reviewed and may be re-organized for online delivery, but are not copy-edited or typeset. Technical support issues arising from supporting information (other than missing files) should be addressed to the authors.

References

Brunig I., Suter A., Knuesel I., Luscher B. and Fritschy J. M. (2002) GABAergic terminals are required for postsynaptic clustering of dystrophin but not of GABA(A) receptors and gephyrin. *J. Neurosci.* **22**, 4805–4813.

Charrier C., Ehrensperger M. V., Dahan M., Levi S. and Triller A. (2006) Cytoskeleton regulation of glycine receptor number at synapses and diffusion in the plasma membrane. *J. Neurosci.* **26**, 8502–8511.

Chen H. I. and Sudol M. (1995) The WW domain of Yes-associated protein binds a proline-rich ligand that differs from the consensus established for Src homology 3-binding modules. *Proc. Natl Acad. Sci. USA* **92**, 7819–7823.

Chen H. J., Rojas-Soto M., Oguni A. and Kennedy M. B. (1998) A synaptic Ras-GTPase activating protein (p135 SynGAP) inhibited by CaM kinase II. *Neuron* **20**, 895–904.

Choi S., Ko J., Lee J. R., Lee H. W., Kim K., Chung H. S., Kim H. and Kim E. (2006) ARF6 and EFA6A regulate the development and maintenance of dendritic spines. *J. Neurosci.* **26**, 4811–4819.

Claing A. (2004) Regulation of G protein-coupled receptor endocytosis by ARF6 GTP-binding proteins. *Biochem. Cell Biol.* **82**, 610–617.

Cox R., Mason-Gamer R. J., Jackson C. L. and Segev N. (2004) Phylogenetic analysis of Sec7-domain-containing Arf nucleotide exchangers. *Mol. Biol. Cell* **15**, 1487–1505.

Delaney K. A., Murph M. M., Brown L. M. and Radhakrishna H. (2002) Transfer of M2 muscarinic acetylcholine receptors to clathrin-derived early endosomes following clathrin-independent endocytosis. *J. Biol. Chem.* **277**, 33439–33446.

Dosemeci A., Makusky A. J., Jankowska-Stephens E., Yang X., Slotta D. J. and Markey S. P. (2007) Composition of the synaptic PSD-95 complex. *Mol. Cell Proteomics* **6**, 1749–1760.

D'Souza-Schorey C. and Chavrier P. (2006) ARF proteins: roles in membrane traffic and beyond. *Nat. Rev. Mol. Cell Biol.* **7**, 347–358.

D'Souza-Schorey C., Li G., Colombo M. I. and Stahl P. D. (1995) A regulatory role for ARF6 in receptor-mediated endocytosis. *Science* **267**, 1175–1178.

Dunphy J. L., Moravec R., Ly K., Lasell T. K., Melancon P. and Casanova J. E. (2006) The Arf6 GEF GEP100/BRAG2 regulates cell adhesion by controlling endocytosis of beta1 integrins. *Curr. Biol.* **16**, 315–320.

Essrich C., Lorez M., Benson J. A., Fritschy J. M. and Luscher B. (1998) Postsynaptic clustering of major GABAA receptor subtypes requires the gamma 2 subunit and gephyrin. *Nat. Neurosci.* **1**, 563–571.

Feng G., Tintrup H., Kirsch J., Nichol M. C., Kuhse J., Betz H. and Sanes J. R. (1998) Dual requirement for gephyrin in glycine receptor clustering and molybdoenzyme activity. *Science* **282**, 1321–1324.

Fritschy J. M., Harvey R. J. and Schwarz G. (2008) Gephyrin: where do we stand, where do we go? *Trends Neurosci.* **31**, 257–264.

Fukaya M. and Watanabe M. (2000) Improved immunohistochemical detection of postsynaptically located PSD-95/SAP90 protein family by protease section pretreatment: a study in the adult mouse brain. *J. Comp. Neurol.* **426**, 572–586.

Fukudome Y., Ohno-Shosaku T., Matsui M. *et al.* (2004) Two distinct classes of muscarinic action on hippocampal inhibitory synapses: M2-mediated direct suppression and M1/M3-mediated indirect suppression through endocannabinoid signalling. *Eur. J. Neurosci.* **19**, 2682–2692.

Giesemann T., Schwarz G., Nawrotzki R. *et al.* (2003) Complex formation between the postsynaptic scaffolding protein gephyrin, profilin, and Mena: a possible link to the microfilament system. *J. Neurosci.* **23**, 8330–8339.

Grady R. M., Wozniak D. F., Ohlemiller K. K. and Sanes J. R. (2006) Cerebellar synaptic defects and abnormal motor behavior in mice lacking alpha- and beta-dystrobrevin. *J. Neurosci.* **26**, 2841–2851.

Gray E. G. (1959) Axo-somatic and axo-dendritic synapses of the cerebral cortex: an electron microscope study. *J. Anat.* **93**, 420–433.

Harvey K., Duguid I. C., Alldred M. J. *et al.* (2004) The GDP-GTP exchange factor collybistin: an essential determinant of neuronal gephyrin clustering. *J. Neurosci.* **24**, 5816–5826.

Hattori Y., Ohta S., Hamada K., Yamada-Okabe H., Kanemura Y., Matsuzaki Y., Okano H., Kawakami Y. and Toda M. (2007) Identification of a neuron-specific human gene, KIAA1110, that is a guanine nucleotide exchange factor for ARF1. *Biochem. Biophys. Res. Commun.* **364**, 737–742.

Hernandez-Deviez D. J., Casanova J. E. and Wilson J. M. (2002) Regulation of dendritic development by the ARF exchange factor ARNO. *Nat. Neurosci.* **5**, 623–624.

Hernandez-Deviez D. J., Roth M. G., Casanova J. E. and Wilson J. M. (2004) ARNO and ARF6 regulate axonal elongation and branching through downstream activation of phosphatidylinositol 4-phosphate 5-kinase alpha. *Mol. Biol. Cell* **15**, 111–120.

Hiroi T., Someya A., Thompson W., Moss J. and Vaughan M. (2006) GEP100/BRAG2: activator of ADP-ribosylation factor 6 for regulation of cell adhesion and actin cytoskeleton via E-cadherin and alpha-catenin. *Proc. Natl. Acad. Sci. USA* **103**, 10672–10677.

Hosaka M., Toda K., Takatsu H., Torii S., Murakami K. and Nakayama K. (1996) Structure and intracellular localization of mouse ADP-ribosylation factors type 1 to type 6 (ARF1–ARF6). *J. Biochem. (Tokyo)* **120**, 813–819.

Houndolo T., Boulay P. L. and Claing A. (2005) G protein-coupled receptor endocytosis in ADP-ribosylation factor 6-depleted cells. *J. Biol. Chem.* **280**, 5598–5604.

Inaba Y., Tian Q. B., Okano A. *et al.* (2004) Brain-specific potential guanine nucleotide exchange factor for Arf, synArfGEF (Po), is localized to postsynaptic density. *J. Neurochem.* **89**, 1347–1357.

Katsumata O., Ohara N., Tamaki H., Niimura T., Naganuma H., Watanabe M. and Sakagami H. (2009) IQ-ArfGEF/BRAG1 is associated with synaptic ribbons in the mouse retina. *Eur. J. Neurosci.* **30**, 1509–1516.

Kins S., Betz H. and Kirsch J. (2000) Collybistin, a newly identified brain-specific GEF, induces submembrane clustering of gephyrin. *Nat. Neurosci.* **3**, 22–29.

Kirsch J. and Betz H. (1995) The postsynaptic localization of the glycine receptor-associated protein gephyrin is regulated by the cytoskeleton. *J. Neurosci.* **15**, 4148–4156.

Kirsch J., Langosch D., Prior P., Littauer U. Z., Schmitt B. and Betz H. (1991) The 93-kDa glycine receptor-associated protein binds to tubulin. *J. Biol. Chem.* **266**, 22242–22245.

Kirsch J., Wolters I., Triller A. and Betz H. (1993) Gephyrin antisense oligonucleotides prevent glycine receptor clustering in spinal neurons. *Nature* **366**, 745–748.

Kneussel M. and Betz H. (2000) Receptors, gephyrin and gephyrin-associated proteins: novel insights into the assembly of inhibitory postsynaptic membrane specializations. *J. Physiol.* **525**(Pt 1), 1–9.

Knuesel I., Mastrocola M., Zuellig R. A., Bornhauser B., Schaub M. C. and Fritschy J. M. (1999) Short communication: altered synaptic clustering of GABAA receptors in mice lacking dystrophin (mdx mice). *Eur. J. Neurosci.* **11**, 4457–4462.

Knuesel I., Bornhauser B. C., Zuellig R. A., Heller F., Schaub M. C. and Fritschy J. M. (2000) Differential expression of utrophin and dystrophin in CNS neurons: an in situ hybridization and immunohistochemical study. *J. Comp. Neurol.* **422**, 594–611.

Krauss M., Kinuta M., Wenk M. R., De Camilli P., Takei K. and Haucke V. (2003) ARF6 stimulates clathrin/AP-2 recruitment to synaptic membranes by activating phosphatidylinositol phosphate kinase type Igamma. *J. Cell Biol.* **162**, 113–124.

Levi S., Grady R. M., Henry M. D., Campbell K. P., Sanes J. R. and Craig A. M. (2002) Dystroglycan is selectively associated with inhibitory GABAergic synapses but is dispensable for their differentiation. *J. Neurosci.* **22**, 4274–4285.

Mammoto A., Sasaki T., Asakura T., Hotta I., Imamura H., Takahashi K., Matsuura Y., Shirao T. and Takai Y. (1998) Interactions of drebrin

and gephyrin with profilin. *Biochem. Biophys. Res. Commun.* **243**, 86–89.

Morishige M., Hashimoto S., Ogawa E. *et al.* (2008) GEP100 links epidermal growth factor receptor signalling to Arf6 activation to induce breast cancer invasion. *Nat. Cell Biol.* **10**, 85–92.

Murphy J. A., Jensen O. N. and Walikonis R. S. (2006) BRAG1, a Sec7 domain-containing protein, is a component of the postsynaptic density of excitatory synapses. *Brain Res.* **1120**, 35–45.

Niwa H., Yamamura K. and Miyazaki J. (1991) Efficient selection for high-expression transfectants with a novel eukaryotic vector. *Gene* **108**, 193–199.

Pak D. T., Yang S., Rudolph-Correia S., Kim E. and Sheng M. (2001) Regulation of dendritic spine morphology by SPAR, a PSD-95-associated RapGAP. *Neuron* **31**, 289–303.

Papadopoulos T., Korte M., Eulenburg V. *et al.* (2007) Impaired GABAergic transmission and altered hippocampal synaptic plasticity in collybistin-deficient mice. *EMBO J.* **26**, 3888–3899.

Peng J., Kim M. J., Cheng D., Duong D. M., Gygi S. P. and Sheng M. (2004) Semiquantitative proteomic analysis of rat forebrain postsynaptic density fractions by mass spectrometry. *J. Biol. Chem.* **279**, 21003–21011.

Penzes P., Johnson R. C., Alam M. R., Kambampati V., Mains R. E. and Eipper B. A. (2000) An isoform of kalirin, a brain-specific GDP/GTP exchange factor, is enriched in the postsynaptic density fraction. *J. Biol. Chem.* **275**, 6395–6403.

Penzes P., Johnson R. C., Sattler R., Zhang X., Huganir R. L., Kambampati V., Mains R. E. and Eipper B. A. (2001) The neuronal Rho-GEF Kalirin-7 interacts with PDZ domain-containing proteins and regulates dendritic morphogenesis. *Neuron* **29**, 229–242.

Pfeiffer F., Graham D. and Betz H. (1982) Purification by affinity chromatography of the glycine receptor of rat spinal cord. *J. Biol. Chem.* **257**, 9389–9393.

Poulopoulos A., Aramuni G., Meyer G. *et al.* (2009) Neuroligin 2 drives postsynaptic assembly at perisomatic inhibitory synapses through gephyrin and collybistin. *Neuron* **63**, 628–642.

Rentschler S., Linn H., Deininger K., Bedford M. T., Espanel X. and Sudol M. (1999) The WW domain of dystrophin requires EF-hands region to interact with beta-dystroglycan. *Biol. Chem.* **380**, 431–442.

Sakagami H., Kamata A., Fukunaga K. and Kondo H. (2005) Functional assay of EFA6A, a guanine nucleotide exchange factor for ADP-ribosylation factor 6 (ARF6), in dendritic formation of hippocampal neurons. *Methods Enzymol.* **404**, 232–242.

Sakagami H., Suzuki H., Kamata A., Owada Y., Fukunaga K., Mayanagi H. and Kondo H. (2006) Distinct spatiotemporal expression of EFA6D, a guanine nucleotide exchange factor for ARF6, among the EFA6 family in mouse brain. *Brain Res.* **1093**, 1–11.

Sakagami H., Honnma T., Sukegawa J., Owada Y., Yanagisawa T. and Kondo H. (2007) Somatodendritic localization of EFA6A, a guanine nucleotide exchange factor for ADP-ribosylation factor 6, and its possible interaction with alpha-actinin in dendritic spines. *Eur. J. Neurosci.* **25**, 618–628.

Sakagami H., Sanda M., Fukaya M. *et al.* (2008) IQ-ArfGEF/BRAG1 is a guanine nucleotide exchange factor for Arf6 that interacts with PSD-95 at postsynaptic density of excitatory synapses. *Neurosci. Res.* **60**, 199–212.

Sanda M., Kamata A., Katsumata O., Fukunaga K., Watanabe M., Kondo H. and Sakagami H. (2009) The postsynaptic density protein, IQ-ArfGEF/BRAG1, can interact with IRSp53 through its proline-rich sequence. *Brain Res.* **1251**, 7–15.

Scannevin R. H. and Huganir R. L. (2000) Postsynaptic organization and regulation of excitatory synapses. *Nat. Rev. Neurosci.* **1**, 133–141.

Scholz R., Berberich S., Rathgeber L., Kolleker A., Kohr G. and Kornau H. C. (2010) AMPA receptor signaling through BRAG2 and Arf6 critical for long-term synaptic depression. *Neuron* **66**, 768–780.

Shinotsuka C., Yoshida Y., Kawamoto K., Takatsu H. and Nakayama K. (2002) Overexpression of an ADP-ribosylation factor-guanine nucleotide exchange factor, BIG2, uncouples brefeldin A-induced adaptor protein-1 coat dissociation and membrane tubulation. *J. Biol. Chem.* **277**, 9468–9473.

Shoubridge C., Tarpey P. S., Abidi F. *et al.* (2010) Mutations in the guanine nucleotide exchange factor gene IQSEC2 cause nonsyndromic intellectual disability. *Nat. Genet.* **42**, 486–488.

Someya A., Sata M., Takeda K., Pacheco-Rodriguez G., Ferrans V. J., Moss J. and Vaughan M. (2001) ARF-GEP(100), a guanine nucleotide-exchange protein for ADP-ribosylation factor 6. *Proc. Natl Acad. Sci. USA* **98**, 2413–2418.

Sumita K., Sato Y., Iida J., Kawata A., Hamano M., Hirabayashi S., Ohno K., Peles E. and Hata Y. (2007) Synaptic scaffolding molecule (S-SCAM) membrane-associated guanylate kinase with inverted organization (MAGI)-2 is associated with cell adhesion molecules at inhibitory synapses in rat hippocampal neurons. *J. Neurochem.* **100**, 154–166.

Takatsu H., Yoshino K., Toda K. and Nakayama K. (2002) GGA proteins associate with Golgi membranes through interaction between their GGAH domains and ADP-ribosylation factors. *Biochem. J.* **365**, 369–378.

Tanabe K., Torii T., Natsume W., Braesch-Andersen S., Watanabe T. and Satake M. (2005) A novel GTPase-activating protein for ARF6 directly interacts with clathrin and regulates clathrin-dependent endocytosis. *Mol. Biol. Cell* **16**, 1617–1628.

Vazquez L. E., Chen H. J., Sokolova I., Knuesel I. and Kennedy M. B. (2004) SynGAP regulates spine formation. *J. Neurosci.* **24**, 8862–8872.

Vitale N., Chasserot-Golaz S., Bailly Y., Morinaga N., Frohman M. A. and Bader M. F. (2002) Calcium-regulated exocytosis of dense-core vesicles requires the activation of ADP-ribosylation factor (ARF)6 by ARF nucleotide binding site opener at the plasma membrane. *J. Cell Biol.* **159**, 79–89.

Woolfrey K. M., Srivastava D. P., Photowala H. *et al.* (2009) Epac2 induces synapse remodeling and depression and its disease-associated forms alter spines. *Nat. Neurosci.* **12**, 1275–1284.

Yamazaki M., Fukaya M., Hashimoto K. *et al.* (2010) TARPs gamma-2 and gamma-7 are essential for AMPA receptor expression in the cerebellum. *Eur. J. Neurosci.* **31**, 2204–2220.

Zhang H., Webb D. J., Asmussen H. and Horwitz A. F. (2003) Synapse formation is regulated by the signaling adaptor GIT1. *J. Cell Biol.* **161**, 131–142.

Zhang H., Webb D. J., Asmussen H., Niu S. and Horwitz A. F. (2005) A GIT1/PIX/Rac/PAK signaling module regulates spine morphogenesis and synapse formation through MLC. *J. Neurosci.* **25**, 3379–3388.

Crosstalk between Glucocorticoid Receptor and Nutritional Sensor mTOR in Skeletal Muscle

Noriaki Shimizu,[1,10] Noritada Yoshikawa,[1,2,10] Naoki Ito,[3,4] Takako Maruyama,[1] Yuko Suzuki,[3] Sin-ichi Takeda,[3] Jun Nakae,[5] Yusuke Tagata,[9] Shinobu Nishitani,[9] Kenji Takehana,[9] Motoaki Sano,[6] Keiichi Fukuda,[6] Makoto Suematsu,[7,8] Chikao Morimoto,[1,2] and Hirotoshi Tanaka[1,2,*]

[1]Division of Clinical Immunology, Advanced Clinical Research Center
[2]Department of Rheumatology and Allergy, Research Hospital
Institute of Medical Science, University of Tokyo, Tokyo 108-8639, Japan
[3]Department of Molecular Therapy, National Institute of Neuroscience, National Center of Neurology and Psychiatry, Kodaira 187-8502, Japan
[4]Department of Biological Information, Tokyo Institute of Technology, Yokohama 226-8501, Japan
[5]Frontier Medicine on Metabolic Syndrome, Division of Endocrinology, Metabolism and Nephrology, Department of Internal Medicine
[6]Cardiology Division, Department of Internal Medicine
[7]Department of Biochemistry
[8]JST ERATO, Suematsu Gas Biology Project
Keio University School of Medicine, Tokyo 160-8582, Japan
[9]Ajinomoto Pharmaceuticals Co., Ltd., Kawasaki 210-8681, Japan
[10]These authors contributed equally to this work
*Correspondence: hirotnk@ims.u-tokyo.ac.jp
DOI 10.1016/j.cmet.2011.01.001

SUMMARY

Maintenance of skeletal muscle mass relies on the dynamic balance between anabolic and catabolic processes and is important for motility, systemic energy homeostasis, and viability. We identified direct target genes of the glucocorticoid receptor (GR) in skeletal muscle, i.e., REDD1 and KLF15. As well as REDD1, KLF15 inhibits mTOR activity, but via a distinct mechanism involving BCAT2 gene activation. Moreover, KLF15 upregulates the expression of the E3 ubiquitin ligases atrogin-1 and MuRF1 genes and negatively modulates myofiber size. Thus, GR is a liaison involving a variety of downstream molecular cascades toward muscle atrophy. Notably, mTOR activation inhibits GR transcription function and efficiently counteracts the catabolic processes provoked by glucocorticoids. This mutually exclusive crosstalk between GR and mTOR, a highly coordinated interaction between the catabolic hormone signal and the anabolic machinery, may be a rational mechanism for fine-tuning of muscle volume and a potential therapeutic target for muscle wasting.

INTRODUCTION

Muscle comprises ~40% of body mass and contributes not only to the structure and movement of the body but also to nutrient storage and supply (Matthews, 1999). In adult mammals, skeletal muscle hypertrophy/atrophy is characterized by an increase/decrease in the size (as opposed to the number) of individual myofibers, respectively. The control of muscle mass is believed to be determined by a dynamic balance between anabolic and catabolic processes (Hoffman and Nader, 2004). Mammalian target of rapamycin (mTOR) is a crucial component of the anabolic machinery for protein synthesis. mTOR consists of two complexes: mTORC1, which includes Raptor, signals to S6K and 4E-BP1, controls protein synthesis, and is rapamycin sensitive; and mTORC2, which includes Rictor, signals to Akt, and is rapamycin insensitive. mTORC1 integrates four major signals: growth factors, energy status, oxygen, and amino acids, especially branched-chain amino acids (BCAAs). Prototypically, insulin/IGF-1 activates mTOR via the PI3K-Akt pathway (Sengupta et al., 2010). It is currently considered that mTORC1, and not mTORC2, is essential for the maintenance of muscle mass and function (Bentzinger et al., 2008; Risson et al., 2009). Protein degradation in skeletal muscle cells is essentially mediated by the activity of two conserved pathways: the ubiquitin-proteasomal pathway and the autophagic/lysosomal pathway (Sandri, 2008). The ubiquitin-proteasomal pathway is responsible for the turnover of the majority of soluble and myofibrillar muscle proteins. The activity of this pathway is markedly increased in atrophying muscle due to the transcriptional activation of a set of E3 ligase-encoding genes, e.g., atrogin-1 and MuRF1 (Glass, 2003; Sandri et al., 2004). Autophagy also plays an important role in the degradation of skeletal muscle, and is indicated to be a consequence of an ordered transcriptional program involving a battery of genes, e.g., LC3 and Bnip3 (Mizushima et al., 2008). These positive and negative pathways are balanced in a highly coordinated manner for the determination of myofiber size and total muscle volume; however, distortion of this balance with a relative increase in degradation results in the generalized decrease of myofiber size and muscle atrophy (Hoffman and Nader, 2004). Pioneering studies demonstrated that muscle atrophy is a result of active processes that are transcriptionally controlled through the expression of a particular gene set; the forkhead box O (FoxO) transcription factors are

common components of a number of atrophy models and act as critical liaison molecules for protein degradation and autophagy via the transcriptional regulation of, for example, atrogin-1, MuRF1, LC3, and Bnip3 (Mammucari et al., 2007; Sandri et al., 2004; Stitt et al., 2004; Zhao et al., 2007). In clear contrast, it is evident that each disease has proper signaling pathways to FoxOs and that other components of the cellular machinery often participate in the progression of atrophy (Moresi et al., 2010; Suzuki et al., 2007). Therefore, for the development of therapies against muscle atrophy, it should be addressed how the transcriptional program triggered by a particular atrophy pathway is orchestrated and how the balance of muscle protein synthesis and degradation is distorted in each disease.

Adrenal glucocorticoids produce their actions via a signal pathway involving the ubiquitously expressed glucocorticoid receptor (GR), a prototypic member of the nuclear receptor superfamily, which acts as a ligand-dependent transcription factor. Upon binding glucocorticoids, GR translocates into the nucleus and binds to the glucocorticoid response element (GRE) in the promoters of target genes. The binding of liganded receptors to target DNA is followed by the recruitment of mediators and coactivators to the proximity of GRE, resulting in the recruitment of RNA polymerase II (RNAPII) to nearby transcription start sites and the activation of transcription (Evans, 2005; Meijsing et al., 2009). In skeletal muscle, glucocorticoids elicit a variety of biological actions in the metabolism of glucose, lipids, and proteins and contribute to metabolic homeostasis (Munck et al., 1984). On the other hand, the prolonged oversecretion or exogenous administration of glucocorticoid gives rise to undesirable effects including muscle atrophy (Munck et al., 1984). Although many studies addressed the mechanism of glucocorticoid-induced muscle atrophy, how the glucocorticoid-GR system generates the functional coupling between metabolic regulation and volume adjustment in skeletal muscle remains unsolved. Of note, many pathological conditions characterized by muscle atrophy, e.g., sepsis, cachexia, starvation, metabolic acidosis, and severe insulinopenia, are associated with an increase in circulating glucocorticoid levels. Adrenalectomy or treatment with the GR antagonist RU486 attenuates muscle atrophy in sepsis, cachexia, starvation, and severe insulinopenia (Menconi et al., 2007; Schakman et al., 2008). Moreover, endogenous glucocorticoids were shown to be essential for muscle atrophy in acute diabetic rodents (Hu et al., 2009). Together, understanding the glucocorticoid-mediated regulation of metabolism-volume coupling in muscle is increasingly important for the management of not only muscle atrophy but also these wasting/metabolic disorders.

Typically, glucocorticoid-induced muscle atrophy is characterized by fast-twitch type II glycolytic muscle fiber loss with reduced or no impact on type I fibers. The mechanism of such fiber specificity is yet unknown. Previous reports suggested that the glucocorticoid-GR system has antianabolic and catabolic effects and promotes degradation via the induction of a set of genes including atrogin-1, MuRF1, and myostatin (Menconi et al., 2007; Schakman et al., 2008). Although the involvement of FoxO transcription factors is reported in the gene regulation of atrogin-1 and MuRF1 under the presence of excess glucocorticoids (Sandri et al., 2004; Stitt et al., 2004), the biochemical role of GR in the transcriptional regulation of muscle tissue has not yet been determined. Therefore, we investigated how GR-mediated gene expression coordinately modulates antianabolic and catabolic actions to understand the functional coupling of metabolism and volume regulation in muscle.

In the present study, we identified REDD1 and KLF15 genes as direct targets of GR. REDD1 is known to be induced by various stressors, including glucocorticoid, and to inhibit mTOR activity via the sequestration of 14-3-3 and the increase of TSC1/2 activity (Wang et al., 2006; DeYoung et al., 2008). We clearly identified the functional GRE via the promoter analysis of REDD1 gene. On the other hand, KLF15 is a recently discovered transcription factor that is involved in several metabolic processes in skeletal muscle; e.g., KLF15 transcriptionally upregulates the gene expression of branched-chain aminotransferase 2 (BCAT2), a mitochondrial enzyme catalyzing the first reaction in the catabolism of BCAA to accelerate BCAA degradation and alanine production in skeletal muscle (Gray et al., 2007). Moreover, phenotypic analysis of cardiac-specific KLF15 knockout mice revealed marked left ventricular hypertrophy, indicating the negative regulatory role of KLF15 on muscle mass (Fisch et al., 2007). We here demonstrated that KLF15 participates in muscle catabolism via the transcriptional regulation of atrogin-1 and MuRF1. Moreover, KLF15 affects mTOR through BCAA degradation and negatively modulates myofiber size. mTOR activation inhibits GR-mediated transcription by suppressing GR recruitment onto target genes, strongly suggesting a mutually exclusive crosstalk between mTOR and GR. Pharmacological activation of mTOR with BCAA attenuated GR-mediated gene expression, leading to the substantial restoration of muscle in glucocorticoid-treated rats. We, therefore, indicate the critical importance of the interaction of GR and mTOR in the regulation of metabolism-volume coupling in skeletal muscle.

RESULTS

REDD1 and KLF15 Are Target Genes of GR in Skeletal Muscle

GR levels were relatively high in type II-rich gastrocnemius and tibialis anterior muscles compared to type I-rich soleus muscle in rats (Figure 1A). Figure 1B illustrates the comparison of the effects of a 3 hr treatment with dexamethasone (DEX) on mRNA expression of various genes between the gastrocnemius and soleus muscles. Hormonal induction of mRNA expression of REDD1, atrogin-1, MuRF1, KLF15, FoxO1, FoxO3, and myostatin, as well as the well-known GR target gene FKBP5 (Yoshikawa et al., 2009), was observed in both muscles, but to a lesser extent in the soleus muscle. Among the genes induced by DEX at 3 hr (Figure 1B), the promoter regions of MuRF1 (Waddell et al., 2008) and myostatin (Ma et al., 2001), but not atrogin-1 (Sandri et al., 2004), contain functional GREs. In addition, REDD1 and KLF15 were also considered as candidates of GR target genes (see the Supplemental Information available online).

Concerning KLF15, we showed, in gastrocnemius muscle and L6 myotubes but not in liver, that KLF15 mRNA and protein expression was induced in a GR-dependent manner (Figure 2A). The promoter region spanning from −4676 to +116 of KLF15 gene was not responsive to DEX; however, the activity of the region spanning −2108 to +1331 was induced by DEX, and

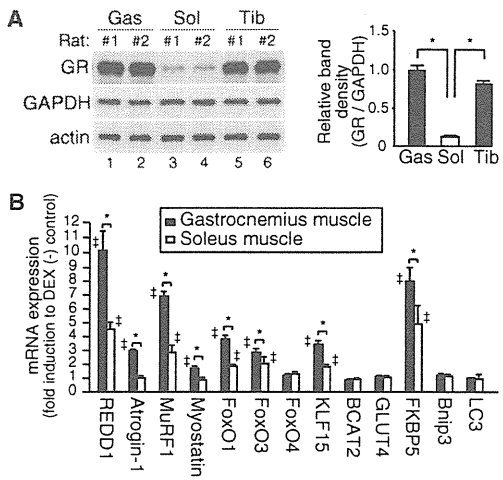

Figure 1. GR Protein Expression and Glucocorticoid-Dependent mRNA Expression of Atrophy-Related Genes in Rat Skeletal Muscles

(A) GR protein levels in rat gastrocnemius (Gas), soleus (Sol), and tibialis anterior (Tib). Left, representative immunoblots. Right, quantified protein levels of GR relative to GAPDH (n = 9).

(B) Induction of mRNA levels of atrophy-related genes by dexamethasone (DEX). Expression levels of the indicated mRNA in the muscles from rats 3 hr after intraperitoneal injection with DEX were assessed in quantitative RT-PCR (qRT-PCR). Results are shown as fold induction to vehicle-treated rats (n = 6).

(A and B) Error bars show SD. *$p < 0.05$, ‡$p < 0.05$ versus vehicle-treated rats.

this induction was inhibited by a GR antagonist RU486. The deletion and mutational analyses of KLF15 promoter indicated that both upper GRE1 and lower GRE2 sites were functional (Figures 2B and 2C). The transient transfection assays using the reporter constructs conveying these minimal GRE sites clearly showed that each GRE is independently functional (Figure 2D). A chromatin immunoprecipitation (ChIP) assay revealed that both GRE-like sequences were targeted by GR and that RNAPII was incorporated onto the coding region of KLF15 gene in the presence of DEX in L6 cells (Figure 2E). We also confirmed the DEX-dependent recruitment of endogenous GR onto the KLF15 promoter in a skeletal muscle-specific manner in vivo (Figure 2F). Similarly, we identified the functional GRE on the REDD1 promoter region and confirmed REDD1 as a GR target gene as well (Figure S1).

KLF15 Transactivates atrogin-1 and MuRF1 Genes

Next, we studied the alteration in the gene expression profile after the direct injection of a KLF15-expressing adenovirus into the rat tibialis anterior muscle. The exogenous expression of KLF15 increased KLF15 protein levels by approximately 5-fold (Figure 3A) and significantly induced mRNA expression of its target gene BCAT2 as anticipated (Figure 3B). Moreover, mRNA expression of atrogin-1, MuRF1, FoxO1, and FoxO3 was stimulated by KLF15 (Figure 3B). We then focused on atrogin-1 and MuRF1 and asked whether the DEX-mediated induction of their mRNA expression was dependent on KLF15. For that purpose, we tested the effect of knocking down the expression of GR or KLF15 on mRNA expression of KLF15, atrogin-1, and MuRF1 as well as another GR target gene REDD1 as a control. In L6 myoblasts, GR knockdown diminished the DEX-dependent mRNA induction of all of these GR target genes. However, KLF15 knockdown affected that of atrogin-1 and MuRF1 but not REDD1 (Figure 3C). These results strongly indicate the critical involvement of the GR-KLF15 cascade in the DEX-mediated upregulation of atrogin-1 and MuRF1 gene expression. To address the role of KLF15 in the transcriptional regulation of atrogin-1 and MuRF1, we constructed luciferase reporter plasmids driven by the promoter of rat atrogin-1 or MuRF1, and tested the effect of the exogenous expression of KLF15 in L6 myoblasts. The expression of the reporter genes was upregulated in a KLF15-dependent manner (Figure 3D). Since the promoter regions of atrogin-1 and MuRF1 contain a number of putative KLF15 recognition sites, we performed ChIP analyses; both promoters had multiple KLF15 binding sites and some of them were located in the proximity of FoxO binding sites and GRE (Figure 3E), and at least one of these KLF15 sites of each promoter recruited KLF15 in a DEX-dependent manner in vivo as well (Figure 3F). Note that atrogin-1 and MuRF1 were originally identified as FoxO target genes (Sandri et al., 2004; Waddell et al., 2008) and that KLF15 induced FoxO mRNA expression (Figure 3B). Indeed, the combination of KLF15 and FoxO significantly enhanced the promoter activity of atrogin-1 and MuRF1 when compared to their individual effects (Figure 3G). Moreover, the direct injection of the adenovirus expressing constitutively active FoxO1 or KLF15 significantly increased atrogin-1 and MuRF1 mRNA expression, and the expression of both resulted in synergistic or additive effects in tibialis anterior (Figure 3H). Therefore, it is likely that KLF15 and FoxO transcription factors cooperatively upregulate the expression of atrogin-1 and MuRF1 genes.

GR-KLF15 Axis Modulates BCAA Metabolism and mTOR Activity

Next, we studied the effects of glucocorticoids, GR, and KLF15 on BCAT2 and BCAA catabolism in skeletal muscle cells. In gastrocnemius muscle, mRNA expression of KLF15 preceded that of BCAT2 after treatment with DEX (Figure 4A). Overexpression of KLF15 increased the BCAT2 promoter-luciferase reporter activity (Figure 4B). Moreover, DEX-induced BCAT2 promoter activation was inhibited by either RU486 or siKLF15 (Figure 4C), indicating that KLF15 is mandatory for GR-mediated BCAT2 gene activation. BCAT2 enzyme activity was stimulated by DEX, and this effect was abolished in the presence of RU486 (Figure 4D). In tibialis anterior muscle and L6 myotubes, the adenovirus-mediated exogenous expression of KLF15 significantly induced BCAT2 enzyme activity even in the absence of DEX (Figure 4E).

The measurement of intracellular amino acid levels clearly revealed the accelerated catabolism of BCAA by KLF15 in myotubes; the exogenous expression of KLF15 decreased the levels of Val, Leu, and Ile, with a reciprocal increase in Ala and Glu without significant alterations in, for example, Gly, Trp, Gln, Tyr, and Phe, in L6 myotubes (Figure 4F). Amino acids, especially BCAA, are believed to activate mTOR and to increase in association with Rheb-mTOR (Sancak et al., 2010). We showed that overexpression of KLF15 in C2C12 myotubes suppressed mTOR activity as demonstrated by the decrease in the phosphorylated form of S6K1. Moreover, mTOR activity was complemented by the addition of excess BCAA (Figure 4G). Of note,

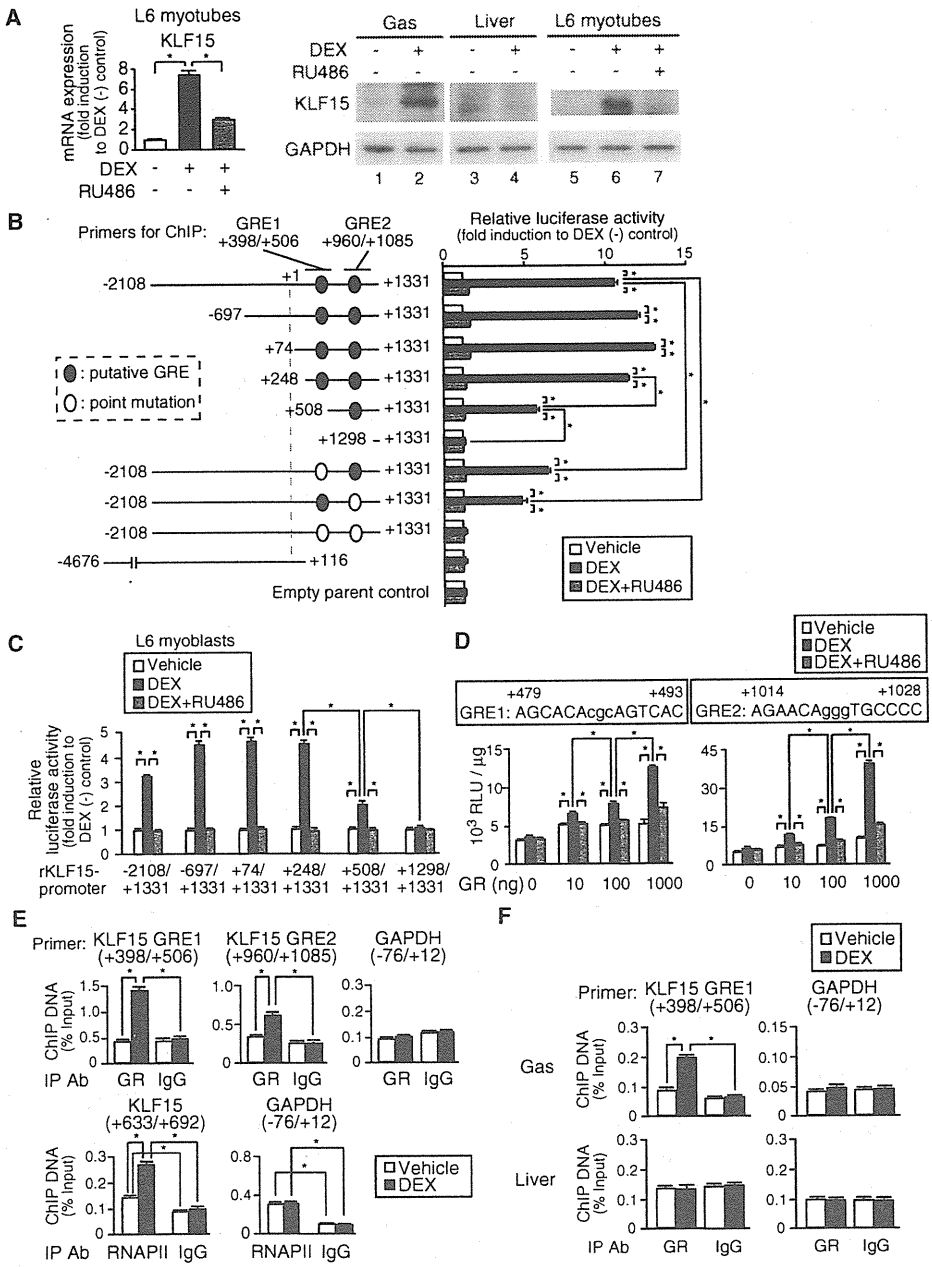

Figure 2. Identification of KLF15 as a Direct GR Target Gene

(A) GR-dependent mRNA (left) and protein (right) expression of KLF15 in L6 myotubes treated with DEX and RU486 for 6 hr and in DEX-treated rat gastrocnemius (see legend for Figure 1B).

(B) Identification of GREs in rat KLF15 promoter. Left, schematic of rat KLF15 promoter-luciferase reporter constructs. Positions of the primers for chromatin immunoprecipitation (ChIP) in (E) and (F) are shown. Right, GR-dependent activation of rat KLF15 promoter-reporter genes. COS-7 cells were transfected with the reporter constructs and 100 ng of GR expression plasmid and treated with DEX and RU486 for 18 hr.

(C) GR-dependent activation of rat KLF15 promoter-reporter genes in L6 myoblasts treated with DEX and RU486 for 18 hr.

(D) GR-dependent activation of reporter genes containing KLF15 promoter GREs. L6 myoblasts were transfected with the luciferase reporter constructs containing the GREs from rat KLF15 with GR expression plasmid and treated with DEX and RU486 for 18 hr.

(E) DEX-dependent recruitment of GR and RNAPII onto rat KLF15 gene. L6 myotubes treated with 1 µM DEX for 2 hr were subjected to ChIP.

(F) Skeletal muscle-specific recruitment of GR onto rat KLF15 gene by DEX. DEX-treated rat gastrocnemius (Gas) and liver (see legend for Figure 1B) were subjected to ChIP.

(A–F) Error bars show SD (n = 5). *p < 0.05.

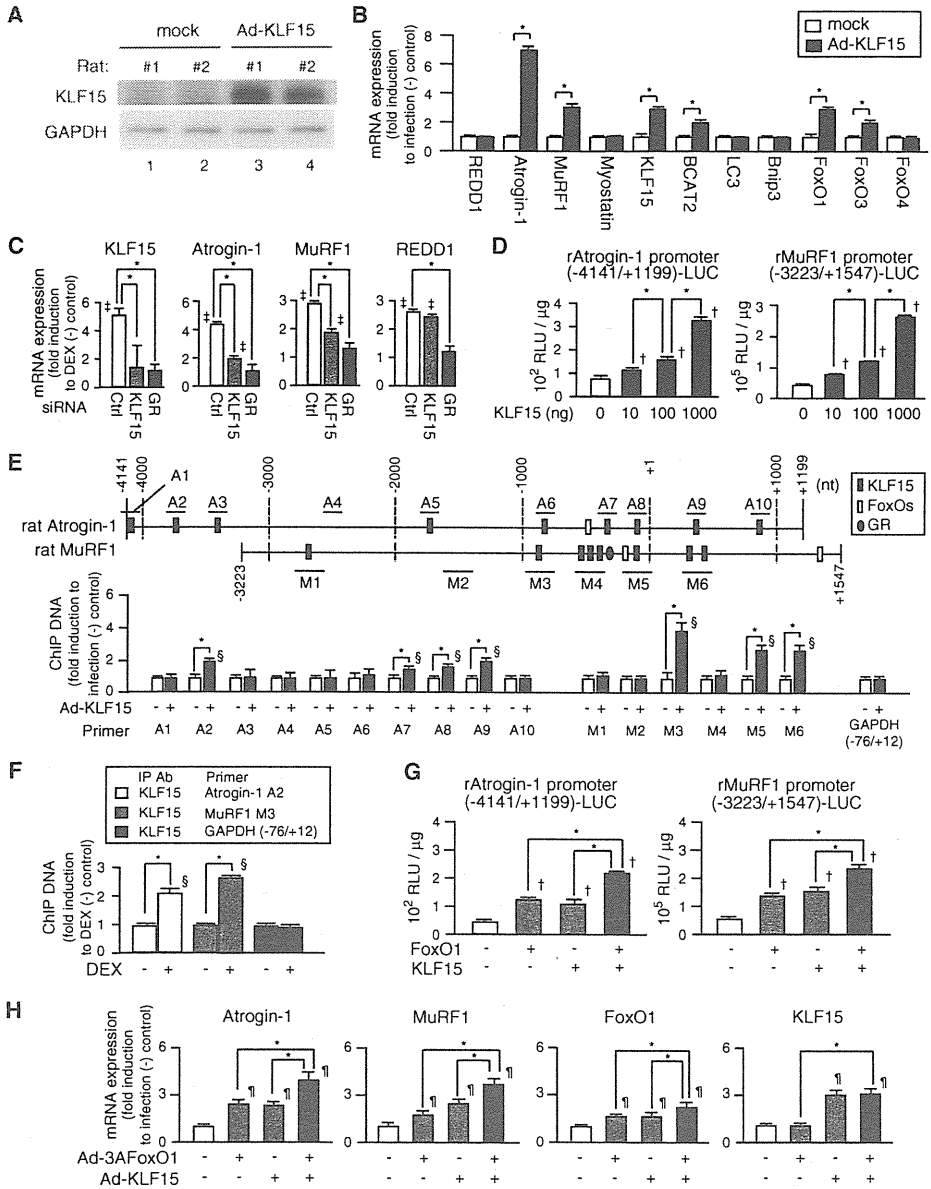

Figure 3. Transcriptional Regulation of Atrogenes by KLF15 and FoxOs

(A and B) KLF15-dependent mRNA expression of atrophy-related genes. Recombinant adenovirus Ad-KLF15 was infected to rat tibialis anterior for 7 days. (A) Immunoblot detection of ectopic KLF15. (B) qRT-PCR.

(C) Effects of knockdown of KLF15 or GR on DEX-dependent mRNA expression of atrophy-related genes. L6 myoblasts were transfected with control siRNA, siRNA against KLF15, or siRNA against GR and treated with DEX for 18 hr.

(D) KLF15-dependent activation of rat atrogin-1 (left) and MuRF1 (right) promoter-reporter genes in L6 myoblasts.

(E) Mapping of the binding sites for KLF15, FoxOs, and GR in rat atrogin-1 and MuRF1 promoters. Top, putative binding sites identified in in silico promoter analysis (see the Experimental Procedures and the Supplemental Information). Bars indicate the positions of the primers for ChIP. Bottom, recruitment of KLF15 onto rat atrogin-1 and MuRF1 promoters. L6 myotubes were infected with Ad-KLF15 for 5 days and subjected to ChIP using anti-KLF15 antibody.

(F) DEX-dependent recruitment of KLF15 onto rat atrogin-1 and MuRF1 promoters in rat gastrocnemius (see Figure 1B).

(G and H) Effects of FoxOs and KLF15 on rat atrogin-1 and MuRF1 promoter-reporter gene expression in L6 myoblasts (G) and on atrogin-1 and MuRF1 mRNA expression in rat tibialis anterior (H). (G) Luciferase assay of L6 myoblasts transfected with the reporter constructs with or without FoxO1 and/or KLF15 expression plasmids. (H) qRT-PCR analysis of rat tibialis anterior expressing ectopic KLF15 and/or constitutive active FoxO1 (3AFoxO1) for 3 days.

(B–H) Error bars show SD (n = 5). *$p < 0.05$, †$p < 0.05$ versus vehicle-treated cells, ‡$p < 0.05$ versus mock-transfected cells, §$p < 0.05$ versus ChIP with normal IgG, ¶$p < 0.05$ versus mock-infected rats.

the diameter of C2C12 myotubes was shortened by KLF15 and rescued by BCAA (Figure 4G). Moreover, exogenous KLF15 reduced mTOR activity with fiber type-independent atrophy in the tibialis anterior muscle (Figure 4H). Taken together, these data indicate that KLF15 is a liaison molecule for GR in the induction of atrogenes and the acceleration of BCAA catabolism and mTOR repression to decrease myofiber size.

mTOR Affects GR-Mediated Transcriptional Regulation

Since little is known about how glucocorticoid-mediated catabolic signal transduction is shut off, we next examined the effects of mTOR blockade using rapamycin on GR-mediated gene expression in L6 myotubes. Surprisingly, rapamycin significantly enhanced the DEX-induced mRNA expression of a number of GR target genes, including REDD1, atrogin-1, MuRF1, KLF15, FoxOs, and FKBP5 (Figure 5A). These results strongly suggest that mTOR blockade selectively enhances mRNA expression of GR target genes, i.e., mTOR activation appears to have a negative impact on GR-mediated gene expression. To further address this negative modulation of GR function by mTOR, we performed transient transfection assays using GR-responsive KLF15 promoter-Luc and GRE-Luc reporter genes in L6 myoblasts. A constitutively active mutant of Rheb, RhebS16H, which autonomously activates mTOR, repressed DEX-mediated reporter gene activation, and rapamycin inhibited these negative effects of RhebS16H (Figure 5B). Moreover, a major endogenous mTOR activator IGF-1 slightly enhanced S6K1 phosphorylation and did not affect DEX-induced GRE-Luc expression when cultured in amino acid-rich media. In clear contrast, in amino acid-deprived media, DEX-dependent induction of GRE-Luc was approximately doubled, and IGF-1 strongly phosphorylated S6K1 and suppressed DEX-induced GRE-Luc expression (Figure 5C). These results indicated that, regardless of the upstream pathways for mTOR activation, endogenous GR activity is negatively controlled by mTOR in L6 myoblasts.

We then asked the underlying mechanisms for mTOR-mediated GR suppression. To test whether mTOR-mediated GR repression is via global protein synthesis downstream of mTOR, we examined luciferase mRNA expression in transient transfection assay using GRE-Luc reporter plasmid in the presence or absence of the protein synthesis inhibitor cycloheximide. Cycloheximide did not influence on either GR-mediated GRE activation or BCAA-mediated GR suppression (Figure 5D). Therefore, BCAA inhibits the transcriptional effects of GR via mTOR activation but not via de novo protein synthesis. Immunoblotting using L6 myotubes revealed that GR protein levels were unaltered in the presence of DEX, BCAA, or rapamycin. Treatment with DEX clearly promoted the nuclear translocation of GR, and such a process was not affected by BCAA or rapamycin (Figure 5E). Concerning the promoter regions spanning the putative GREs in KLF15 and REDD1, DEX-induced GR recruitment was significantly enhanced by rapamycin, suggesting that mTOR negatively influences the access of GR to these promoters. Such an enhancement of GR promoter binding by rapamycin was paralleled by RNAPII recruitment onto the coding regions of KLF15 and REDD1 (Figure 5F). Thus, cellular mTOR activity negatively modulates GR transcriptional function, most possibly by altering the intranuclear behavior of GR. We finally examined the effect of constitutive mTOR activation by studying the impact of adeno-associated virus-driven RhebS16H expression on S6K1 activity and the gene expression profile of the tibialis anterior muscle from DEX-treated rats. RhebS16H-injected muscle had elevated levels of S6K1 phosphorylation and significant decreases in the induction response to DEX of a number of glucocorticoid-inducible genes, including REDD1, atrogin-1, MuRF1, FoxOs, KLF15, and FKBP5, when compared to mock-injected muscle (Figures 5G and 5H).

mTOR Activation Attenuates Glucocorticoid-Induced Muscle Atrophy

It should be noted that numerous studies examined the effects of BCAA on mTOR activity in glucocorticoid-induced atrophy models with conflicting results, the reason for which might be variations in the protocols used in those in vivo studies (Menconi et al., 2007; Schakman et al., 2008). We showed that the bolus administration of a BCAA cocktail via a gastric tube just before the peritoneal injection of DEX (Supplemental Information) resulted in sufficient and reproducible mTOR activation in the gastrocnemius muscle; the phosphorylated form of S6K1 was increased at 30 min after BCAA administration and returned to the baseline level after 90–180 min, even in the presence of DEX (Figure 6A). We then tested the effects of DEX, BCAA, and rapamycin on the protein levels and phosphorylation status of mTOR and its downstream effectors S6K1 and 4E-BP1 as well as Akt, the upstream activator of mTOR, in the rat glucocorticoid-induced atrophy model (5 day intraperitoneal DEX administration, see the Supplemental Information). In GR-rich gastrocnemius muscle, treatment with DEX suppressed the phosphorylation of S6K1 and 4E-BP1, without a significant alteration in p-Akt, indicating that DEX inhibited mTOR function in an Akt-independent fashion in this model. In clear contrast, in either the soleus muscle or liver, DEX treatment did not affect mTOR activity. When BCAA was supplemented, the levels of p-S6K1 and p-4E-BP1 were efficiently restored. Of note, rapamycin canceled these effects of BCAA (Figure 6B). In this model, BCAA administration suppressed the glucocorticoid-induced expression of REDD1, atrogin-1, MuRF1, KLF15, FoxOs, and FKBP5 mRNA (Figure 6C), and there was a decrease in GR recruitment onto the promoters of KLF15, REDD1, MuRF1, and FKBP5 (Figure 6D). BCAA administration also repressed the expression of BCAT2, GLUT4, Bnip3, and LC3 mRNA, and treatment with rapamycin inhibited the effects of BCAA (Figure 6C). In contrast, in the soleus muscle, treatment with DEX alone or DEX plus BCAA only marginally influenced mTOR activity and the gene expression profile, if at all (Figures 6B and 6C).

In this glucocorticoid-induced muscle atrophy rat model, there was a decrease in the body weight of the DEX, DEX plus BCAA, and DEX plus BCAA plus rapamycin groups (Figure 7A). The DEX plus BCAA group revealed a significant restoration of muscle strength as determined by a grip test and the weight of the gastrocnemius muscle when compared with DEX group (Figures 7B and 7C). Histological examination of the gastrocnemius muscle demonstrated typical type II fiber-dominant atrophy in the DEX group; however, the DEX plus BCAA group showed less impairment in the gastrocnemius muscle that was represented by the prevention of type II fiber loss. Semiquantitative analysis using cross-sectional area (CSA) analysis of myofibers strongly supported this notion; the leftward shift in myofiber size

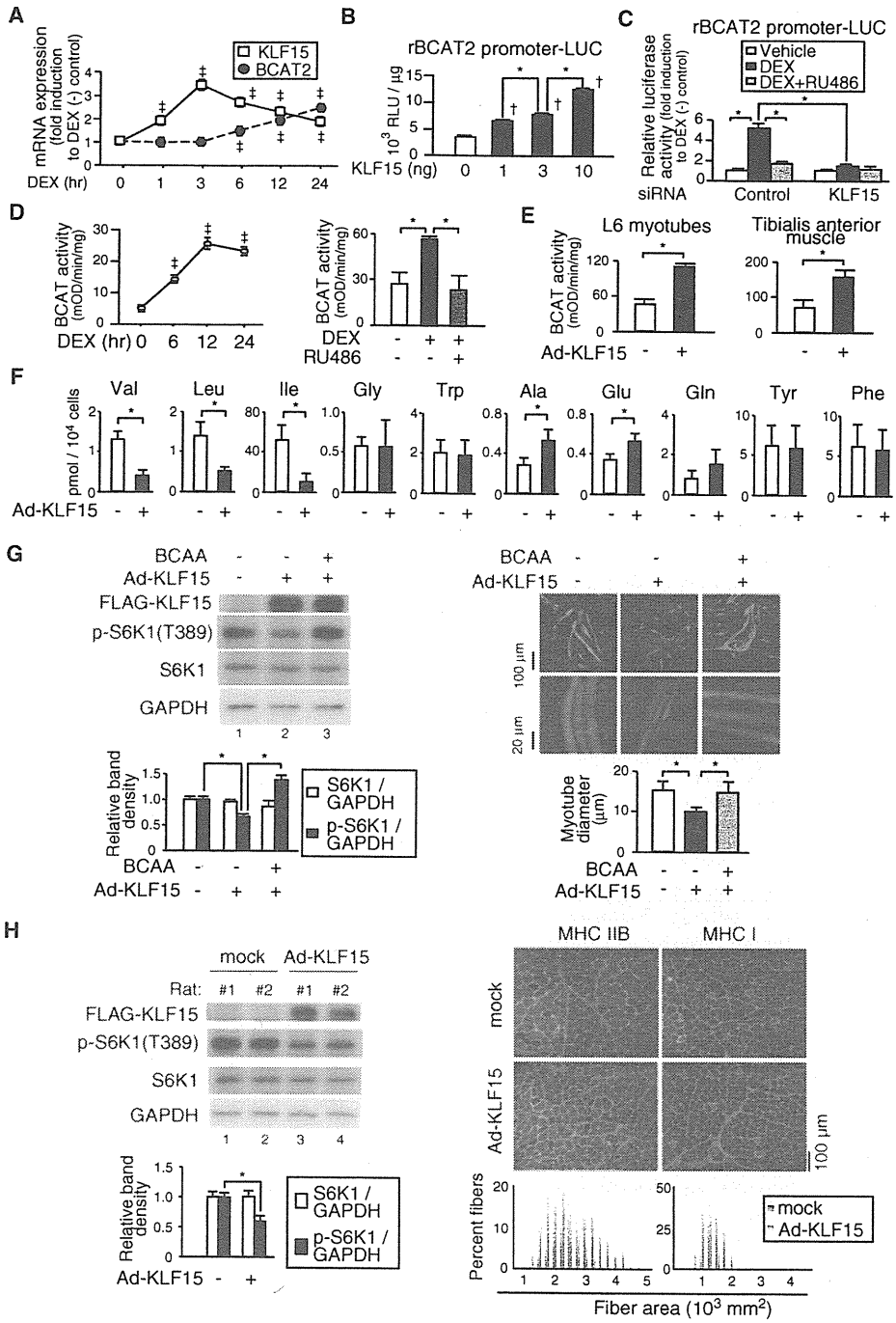

Figure 4. KLF15-Mediated Modulation of BCAA Metabolism and Myofiber Size

(A) Time course of mRNA expression of KLF15 and BCAT2 in rat gastrocnemius after intraperitoneal DEX-injection (n = 5).

(B) KLF15-dependent activation of rat BCAT2 promoter-reporter gene expression in L6 myoblasts (n = 5).

(C) Diminished GR-dependent activation of rat BCAT2 promoter-reporter gene by knockdown of KLF15 in L6 myoblasts (n = 5).

(D) GR-dependent activation of BCAT activity in rat gastrocnemius. Rats were treated with RU486 and/or DEX for the indicated time periods (left) or 6 hr (right) and subjected to BCAT activity measurement as described in the Supplemental Information (n = 5).

(E) KLF15-dependent activation of BCAT activity (n = 5).

(F) Effects of ectopic KLF15 on intracellular amino acid concentrations. L6 myotubes were infected with Ad-KLF15 for 2 days, cultured in amino acid-deprived DMEM for 24 hr, and subjected to quantification of intracellular amino acids as described in the Supplemental Information (n = 3).

(G) Effects of KLF15 and BCAA on mTOR activity and myotube diameter. C2C12 myotubes were infected with GFP-expressing adenovirus and Ad-KLF15 for 2 days and further cultured in amino acid-deprived DMEM supplemented with or without 10 mM BCAA cocktail for 24 hr. Left, representative immunoblots

was observed in the DEX group, but not in the DEX plus BCAA group. In contrast, there was no significant difference in the size of slow type I fibers among the three treatment groups. Moreover, the therapeutic effects of BCAA were inhibited by rapamycin (Figures 7B–7E). Therefore, we conclude that the administration of BCAA elicits mTOR activation and intervenes in GR-dependent catabolic transcriptional regulation to ameliorate DEX-induced muscle atrophy.

DISCUSSION

In skeletal muscle, we suggested that GR activates a secondary transcription network driven by KLF15; that the promoter regions of atrogin-1 and MuRF1 contain KLF15 binding sites as well as those of FoxOs; and that KLF15 induces the expression of these atrogenes. Although the molecular mechanism remains elusive, the functional cooperativity of GR, FoxOs, and KLF15 in the expression of the atrogenes may represent the molecular basis for the involvement of GR in muscle atrophy associated with a number of pathological conditions including diabetes and sepsis. From the metabolic viewpoint, these GR-driven transcriptional cascades appear to be relevant for providing rapid and integrated cues toward muscle breakdown and nutrient supply from muscle to other organs, i.e., to the liver, under stressful conditions associated with excess levels of glucocorticoids.

BCAT2 catalyzes the initial step for BCAA degradation, and BCAT2 activity is a critical determinant of cellular BCAA content in skeletal muscle; mice with systemic inactivation of BCAT2 gene are reported to have approximately ten times or higher concentrations of plasma BCAA (She et al., 2007). We demonstrated that BCAA content was decreased with a reciprocal increase in alanine levels in L6 myotubes after the exogenous expression of KLF15 (Figure 4F). Although it is generally known that BCAA is supplied via protein breakdown during skeletal muscle atrophy (Wagenmakers, 1998; Yu et al., 2010), it was reported that net increase in muscle BCAA concentrations after glucocorticoid treatment (~150% increase compared to control) were strikingly lower than those of diabetic rats (~400% increase compared to control) (Aftring et al., 1988; Hundal et al., 1991). This difference in BCAA concentrations is most likely to be due to increased BCAT2 activity in glucocorticoid-treated rats. The glucocorticoid-driven GR-KLF15-BCAT2 axis may negatively modulate the intracellular availability of BCAA and result in a negative impact on mTOR function in skeletal muscle. Indeed, exogenous KLF15 increased mRNA expression of the atrogenes and BCAT2 and decreased mTOR activity and BCAA concentrations in cultured myotubes (Figures 4E–4G). Moreover, the introduction of KLF15 decreased myofiber size in cultured myotubes and caused atrophy in the tibialis anterior muscle, even in the absence of glucocorticoids (Figures 4G and 4H). Therefore, we may conclude that KLF15 is a crucial GR target gene acting as a catabolic modulator of skeletal muscle.

In addition to the KLF15-BCAT2 axis, it should be noted that a number of glucocorticoid-induced products can repress mTOR activity in skeletal muscle cells. Among others, myostatin (Ma et al., 2001; Gilson et al., 2007) and REDD1 (Figure S1) (DeYoung et al., 2008) are direct targets of GR. Moreover, atrogin-1 was recently reported to inhibit S6K1 activity via eIF3f (Csibi et al., 2010). Therefore, it is likely that the mTOR system is negatively regulated by a variety of factors in the presence of excess glucocorticoids in a distinct fashion. Given that the glucocorticoid-GR axis is a major catabolic regulator for homeostatic control (Munck et al., 1984), this multimodal repression of mTOR via the GR axis appears to be rational. In any case, this type of negative mTOR modulation is not reported in other types of muscle atrophy, and may be a striking feature in glucocorticoid-induced muscle atrophy. Interestingly, muscle-specific inactivation of mTOR was reported to exacerbate the myopathic features of type I and type II fiber-rich muscles in a distinct fashion; type I fiber-rich muscles showed prominent dystrophic features with less impact on muscle mass and CSA compared to type II fiber-rich muscles, and a decrease in muscle mass and CSA are characteristic of type II fiber-rich muscles with less dystrophic appearance (Bentzinger et al., 2008; Risson et al., 2009). Therefore, we speculate that type II fiber-rich glycolytic muscles have an evolutionally preserved role for the storage of nutrients under the control of the glucocorticoid-GR axis and that the GR-triggered gene expression program is a purposeful and efficient compensatory mechanism for nutrient supply from those muscles.

An important question is how the GR-driven proteolytic cascades can be shut down when necessary in skeletal muscle. We clearly demonstrated that mTOR activation negatively modulated GR-mediated transcription. Given that the effect of mTOR is rapamycin sensitive, the involvement of mTORC1 is strongly indicated in this interaction. The role of the mTOR pathway in the determination of glucocorticoid sensitivity has not yet been highlighted, except in certain hematologic malignancies (Beesley et al., 2009; Gu et al., 2008; Yan et al., 2006a). It was postulated that the treatment of cultured cells with FK506 or rapamycin enhances glucocorticoid-inducible reporter gene expression, most possibly via their interaction with heat shock proteins and the promotion of the ligand-dependent nuclear entry of GR (Ning and Sanchez, 1993). In contrast, we documented that rapamycin, without any alteration in the cytoplasmic-nuclear distribution of GR, increased GR recruitment onto the promoter (Figures 5E and 5F), and these effects were not reproduced by FK506 (data not shown).

and quantified band densities of S6K1 and p-S6K1(T389) relative to GAPDH (n = 5). Right, representative fluorescent microscopic images of the myotubes and quantified diameters of the myotubes (500 < n < 510).

(H) Effects of ectopic KLF15 expression on mTOR activity and myofiber cross-sectional area (CSA) in rat tibialis anterior. Left, representative immunoblots and quantified band densities (n = 5). Right, immunostaining for type IIB myosin heavy chain (MHC IIB, red in left photographs), type I myosin heavy chain (MHC I, red in right photographs), and type IV collagen (green) of transverse cryosections. CSA distribution of MHC IIB fibers (left) and MHC I fibers (right) are presented as frequency histograms (500 < n < 510).

(A–H) Error bars show SD. $^{*}p < 0.05$, $^{\ddagger}p < 0.05$ versus vehicle-treated rats. $^{\dagger}p < 0.05$ versus mock-transfected cells.

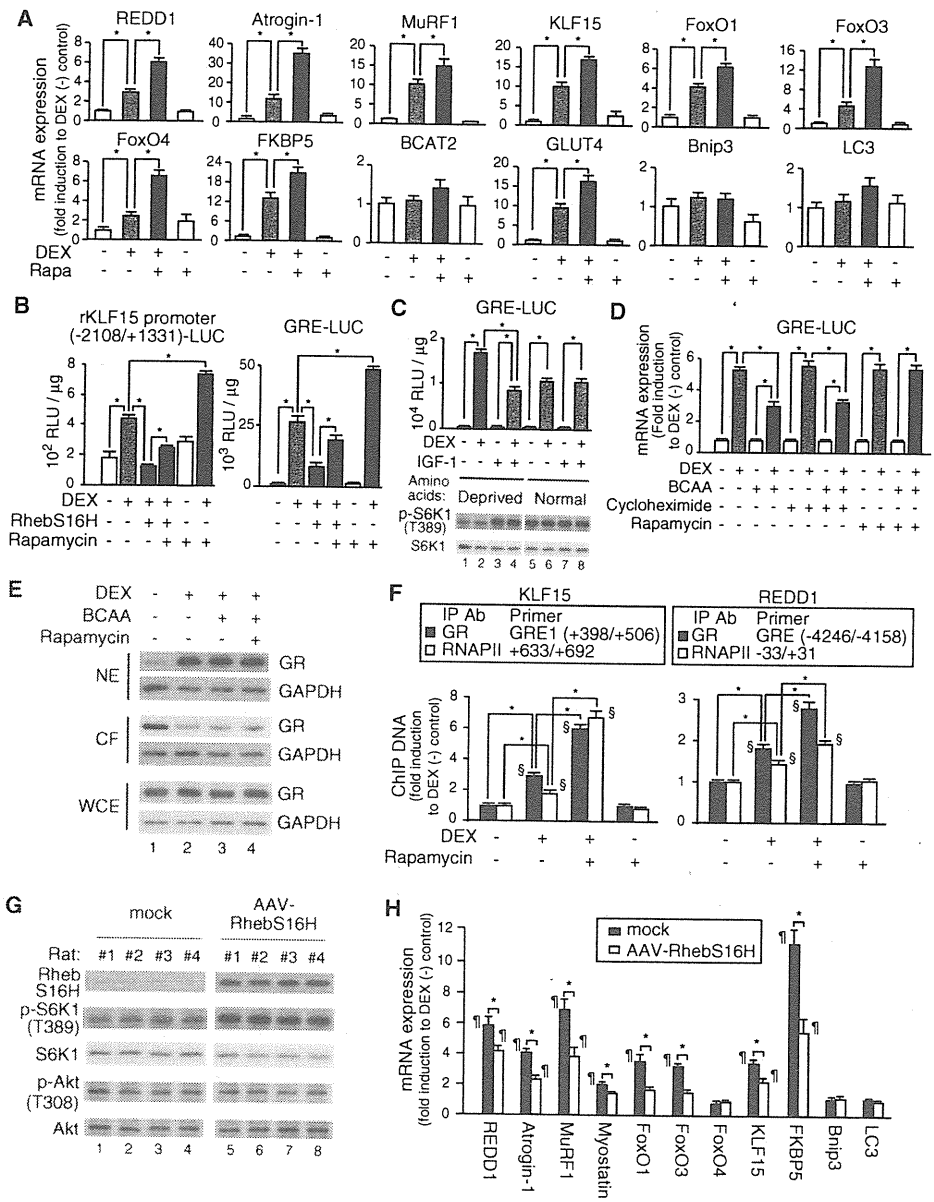

Figure 5. Negative Regulation of GR-Mediated Transcription by mTOR

(A) qRT-PCR analysis of L6 myotubes treated with DEX and rapamycin (Rapa) for 24 hr.

(B) Attenuation of GR-dependent reporter gene expression by mTOR. L6 myoblasts were transfected with rKLF15 promoter-LUC or GRE-LUC, with or without the expression plasmid for a constitutive active Rheb (RhebS16H), and treated with DEX and rapamycin for 18 hr.

(C) Effects of IGF-1 on mTOR activity and GR-dependent reporter gene expression. L6 myoblasts were transfected with GRE-LUC and cultured in amino acid-deprived DMEM (lanes 1–4) or normal DMEM (lanes 5–8) in the presence or absence of IGF-1 and/or DEX for 9 hr. Top, luciferase activities. Bottom, representative immunoblots.

(D) Effects of DEX, BCAA, cycloheximide, and rapamycin on GR-dependent reporter gene expression. L6 myoblasts were transfected with GRE-LUC and cultured in amino acid-deprived DMEM in the presence or absence of 10 mM BCAA cocktail, cycloheximide, rapamycin, and DEX for 6 hr.

(E) Effects of DEX, BCAA, and rapamycin on protein levels and subcellular localization of GR. L6 myotubes were cultured in amino acid-deprived DMEM in the presence or absence of DEX, 10 mM BCAA cocktail, and rapamycin for 30 min. Representative immunoblots of the nuclear extracts (NE), cytoplasmic fractions (CF), and whole-cell extracts (WCE) are shown (n = 3).

(F) Effects of rapamycin on DEX-dependent recruitment of GR onto target gene promoters. L6 myotubes were treated with 1 μM DEX and rapamycin for 2 hr (for KLF15) or 20 min (for REDD1) and processed for ChIP assays.

(G and H) Effects of ectopic expression of RhebS16H on mTOR activity and DEX-mediated mRNA expression. AAV-RhebS16H was infected to rat tibialis anterior for 7 days. (G) Representative immunoblots (n = 7). (H) qRT-PCR analysis of the muscles from the rats 6 hr after intraperitoneal injection with DEX.

(A–D, F, and H) Error bars show SD (n = 5). *$p < 0.05$, §$p < 0.05$ versus ChIP with normal IgG, ¶$p < 0.05$ versus vehicle-treated rats.

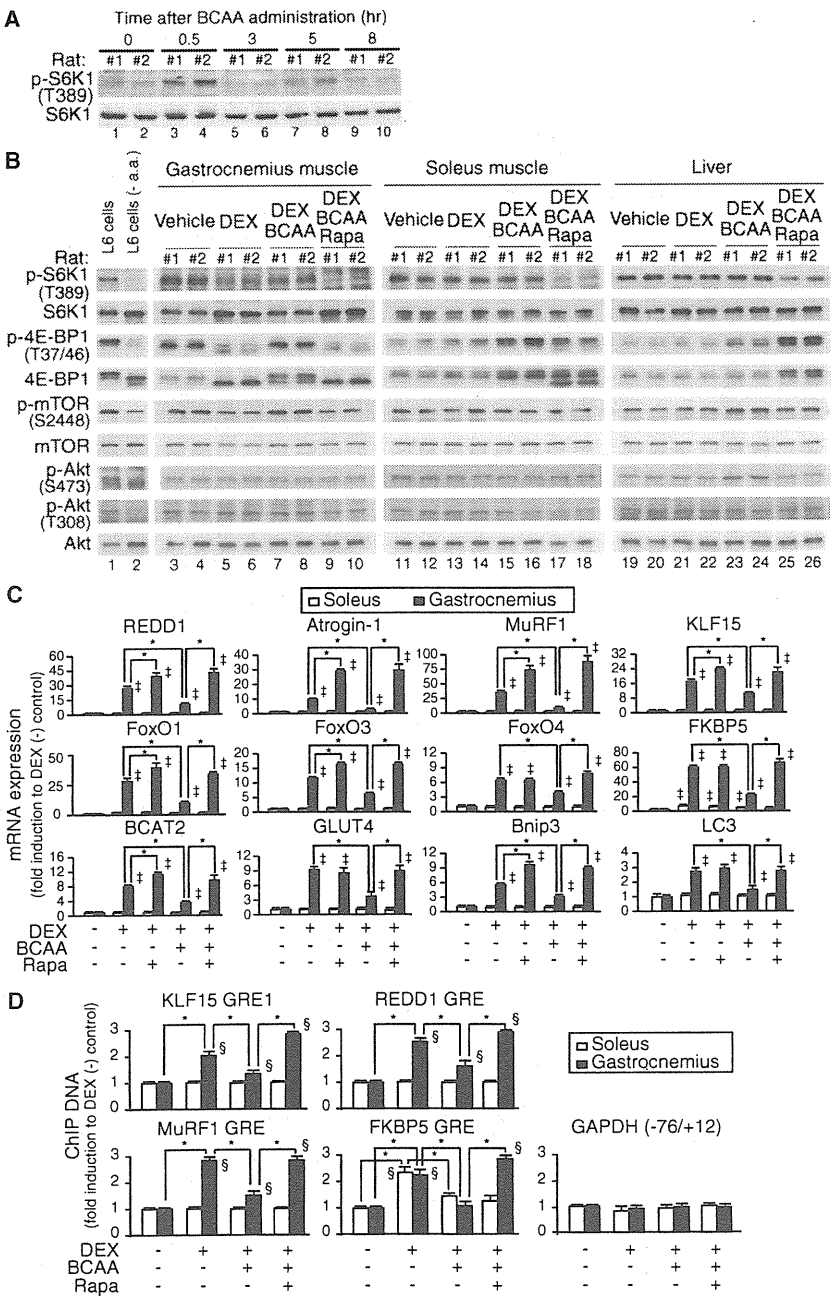

Figure 6. In Vivo Activation of mTOR and Attenuation of GR-Mediated Transcription after Programmed Administration of BCAA

(A) Time course of mTOR activity in rat gastrocnemius after BCAA administration. Representative immunoblots are shown (n = 5).

(B–D) Effects of DEX, BCAA, and rapamycin on mTOR activity; mRNA expression of atrophy-related genes; and GR recruitment onto the target gene promoters. Rats were treated with DEX, BCAA cocktail, and rapamycin for 5 days as described in the Supplemental Information. (B) Representative immunoblots (n = 17). L6 myotubes cultured in normal DMEM and in amino acid-deprived DMEM (–a.a.) for 1 hr were served as controls. (C) mRNA expression of atrophy-related genes. (D) Recruitment of GR onto its target genes. ChIP was performed using anti-GR antibody.

(C and D) Error bars show SD (n = 17). $^{*}p < 0.05$, $^{\ddagger}p < 0.05$ versus vehicle-treated rats, $^{\S}p < 0.05$ versus ChIP with normal IgG.

In skeletal muscle, this nutrition sensor-driven inhibition of GR function may be one of the mechanisms by which nutrients modulate the internal cellular milieu. Intriguingly, GR-mediated transcription was not repressed by insulin/IGF-1 under normal culture conditions, but did so when amino acids were deprived from the culture media (Figure 5C). This indicates that mTOR may be constitutively activated to a certain extent by nutrients and growth factors to protect cells from GR-driven catabolism in skeletal muscle. Under fasting conditions, however, blood concentrations of insulin/IGF-1 are low, and glucocorticoids may be allowed to efficiently drive the catabolic atrophy program for nutrient supply. Thus, our hypothesis may provide an insight into how muscle cells critically determine their volume after sensing endocrine hormones and the nutritional conditions for homeostatic regulation. In this context, GR-mTOR crosstalk might be a key for creating an interdisciplinary research area that bridges nutrition and medicine.

Therefore, the mTOR-mediated inhibition of GR in skeletal muscle is likely to be due not to the modulation of its chaperone activity but to its intervention in the access of GR to target DNA. It is becoming apparent that mTOR is intimately involved with the transcriptional apparatus in concert with a variety of transcription factors and cofactors (Cunningham et al., 2007). Since mTOR is reported to dock in the nucleus in association with, for example, PML (Bernardi et al., 2006), it would be of particular interest to identify such a factor that tethers GR and mTOR in the nucleus.

The biochemical rationale for the usage of BCAA as a therapeutic tool in glucocorticoid-induced muscle atrophy is that BCAA increases the association between Rheb and mTOR and, at least in part, mimics the effect of Rheb overexpression (Sancak et al., 2010). In our model, BCAA administration repressed mRNA expression of almost all GR-regulated genes (Figure 6C). ChIP analysis strongly supported the notion that BCAA administration inhibited GR recruitment onto the promoters of its target genes (Figure 6D). Moreover, these effects of BCAA were efficiently counteracted by rapamycin.

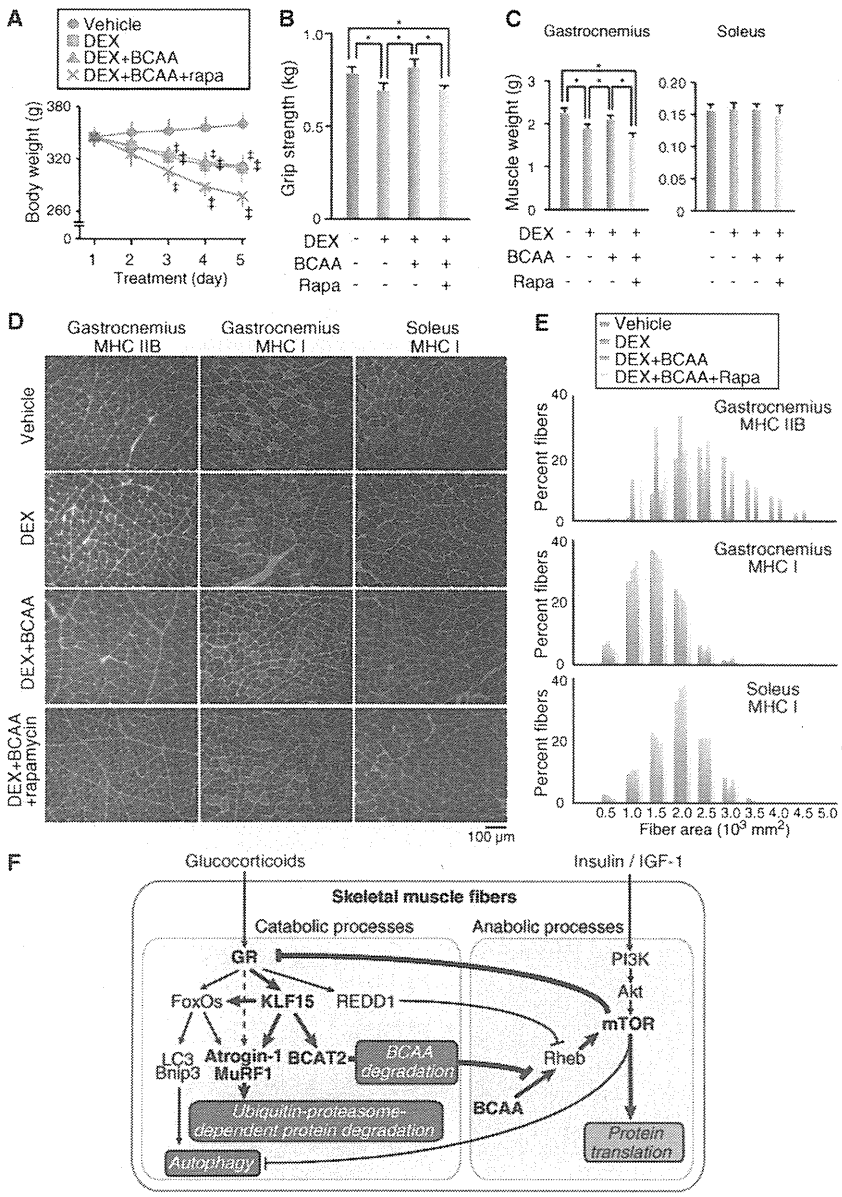

Figure 7. Restoration of Muscle Fiber Mass and Strength by mTOR Activation in DEX-Induced Skeletal Muscle Atrophy Model

(A–E) Effects of DEX, BCAA, and rapamycin on body weight (A), grip strength of forearms (B), muscle weight (C), muscle pathology (D), and CSA of skeletal muscle fiber (E). Rats were treated with DEX, BCAA, and rapamycin for 5 days as described in the Supplemental Information. (A) Time course of body weight ($n = 15$). (B) Grip strength of forearms at 5 hr after DEX injection on the day 5 ($47 < n < 51$). (C) Weight of gastrocnemius and soleus at 6 hr after DEX injection on the day 5 ($n = 15$). (D) Immunostaining for MHC IIB (red in left photographs), MHC I (red in middle and right photographs), and type IV collagen (green) of transverse cryosections. (E) CSA distribution of MHC IIB fibers (gastrocnemius) and MHC I fibers (gastrocnemius and soleus) presented as frequency histograms ($500 < n < 510$). (F) Schematic model of mutual crosstalk between catabolic processes and anabolic processes in skeletal muscle.

(A–C) Error bars show SD (A and C) or SEM (B). $^{*}p < 0.05$, $^{\ddagger}p < 0.05$ versus vehicle-treated rats.

Therefore, we are convinced that the therapeutic effects of BCAA could, at least in part, be ascribed to GR inhibition by the BCAA-mediated activation of mTOR. BCAA administration also resulted in the decreased mRNA expression of autophagy-related genes (Figure 6C), indicating that this therapeutic regimen repressed the vicious circuit connecting the initial induction of GR-triggered gene expression to degradation and atrophy. Of course, we cannot rule out other mechanisms for the effects of BCAA, including the non-GR-mediated repression of atrophy and/or autophagy, and further studies are clearly needed to clarify this issue.

There are conflicting results concerning the biological effects of BCAA, e.g., the overactivation of amino acid-dependent mTOR-mediated signaling can lead to the inhibition of the proximal part of the insulin signaling pathway (Um et al., 2006). Moreover, in obese humans, BCAA in association with a high-fat diet is linked to the elevation of insulin resistance (Newgard et al., 2009). On the other hand, it is suggested that an increase in type II fibers in obese mice may reduce fat mass and improve metabolic parameters (Izumiya et al., 2008). Therefore, it is necessary, for the validation of BCAA therapy, to evaluate the influence of long-term BCAA administration on various metabolic parameters.

In conclusion, we revealed that GR and mTOR act as catabolic and anabolic liaisons for skeletal muscle metabolism, respectively, and these molecules interact with each other at multiple levels. This issue would be of particular importance to understand the molecular mechanism underlying the regulation of the volume and metabolism of muscle and for the development of treatments for glucocorticoid-induced and wasting disorder-related skeletal muscle atrophy.

EXPERIMENTAL PROCEDURES

Rats

All animal experiments were approved by the institutional committee and conducted according to the institutional ethical guidelines for animal experiments. Rapamycin, RU486, the BCAA cocktail, and DEX administration were performed as described in the Supplemental Information. Excised tissues were snap frozen in isopentane cooled by liquid nitrogen, and crushed using Cryo-Press (Microtec, Funabashi, Japan) prefrozen in liquid nitrogen, or processed to serial 10 μm transverse cryostat sections.

Cell Culture

L6 rat myoblasts, C2C12 mouse myoblasts, and COS-7 cells were obtained from American Type Culture Collection (Manassas, VA) and maintained in DMEM supplemented with 10% fetal bovine serum (Invitrogen, Carlsbad, CA). Culture conditions for myotube formation, drug treatment, and amino acids deprivation are described in the Supplemental Information.

In Silico Promoter Analysis

Putative FoxO1- and FoxO3-binding sequences, as well as putative GREs which are conserved between rat and human genomes, were searched for in the genomic regions (−5000 to +2000) of KLF15, REDD1, atrogin-1, and MuRF1 using rVISTA 2.0 as described in the Supplemental Information. KLF15-binding sequences (see the Supplemental Information) were searched for in the promoters of rat atrogin-1 (−4141 to +1191) and MuRF1 (−3223 to +1547) genes.

Chromatin Immunoprecipitation Assay

Cells or crushed tissues were treated with 1% formaldehyde in PBS for 10 min at 37°C, incubated in 125 mM glycine for 5 min, resuspended in buffer S (50 mM Tris [pH 8.0], 1% SDS, 10 mM EDTA) supplemented with 1 mM DTT, 100 nM MG132, and protease and phosphatase inhibitor cocktail (Nacalai Tesque, Kyoto, Japan), and incubated at 10°C for 10 min. Samples were sheared to an average size of 500 bp by sonication. Lysates corresponding to 2×10^6 cells or 200 mg of crushed tissues were diluted 10-fold in buffer D (0.01% SDS, 1.1% Triton X-100, 1.2 mM EDTA, 16.7 mM Tris [pH 8.1], 167 mM NaCl) supplemented with 100 nM MG132, and protease and phosphatase inhibitor cocktail, and incubated with 5 μg of antibodies listed in the Supplemental Information at 4°C for 18 hr. Protein A or G agarose/salmon sperm DNA (Millipore, Billerica, MA) was added and further incubated at 4°C for 1 hr. Precipitated DNA were quantified as described in the Supplemental Information.

Indirect Immunofluorescent Staining and Fluorescence Imaging

Muscle cryosections were treated with 0.1% Triton X-100, blocked with 5% goat serum/1% BSA in PBS, and incubated with antibodies listed in the Supplemental Information. After washing with PBS, specimens were incubated with secondary antibodies labeled with Alexa Fluor 488 or Alexa Fluor 568 (Invitrogen, 1:1000) and analyzed as described in the Supplemental Information. For imaging cultured myotubes, GFP was expressed in myotubes by infecting 10 multiplicity of infection of Ax1CAgfp (RIKEN DNA Bank, Tsukuba, Japan).

Statistical Analysis

Data were analyzed with Student's t test for unpaired data. P values below 0.05 were considered statistically significant. Graphs represent means ± SD or means ± SEM as specified in each figure legend.

SUPPLEMENTAL INFORMATION

Supplemental Information include one figure, Supplemental Experimental Procedures, and Supplemental References and can be found with this article at doi:10.1016/j.cmet.2011.01.001.

ACKNOWLEDGMENTS

This work was supported by Grants-in-Aid for Scientific Research, (to H.T., N.S., and N.Y.) and by grants from the Ministry of Health, Labour, and Welfare and from Japan Science and Technology Agency, Japan (to H.T.). Y.T., S.N., and K.T. are employees of Ajinomoto Pharmaceutical Company.

Received: June 17, 2010
Revised: October 14, 2010
Accepted: December 30, 2010
Published: February 1, 2011

REFERENCES

Aftring, R.P., Miller, W.J., and Buse, M.G. (1988). Effects of diabetes and starvation on skeletal muscle branched-chain alpha-keto acid dehydrogenase activity. Am. J. Physiol. *254*, E292–E300.

Beesley, A.H., Firth, M.J., Ford, J., Weller, R.E., Freitas, J.R., Perera, K.U., and Kees, U.R. (2009). Glucocorticoid resistance in T-lineage acute lymphoblastic leukaemia is associated with a proliferative metabolism. Br. J. Cancer *100*, 1926–1936.

Bentzinger, C.F., Romanino, K., Cloetta, D., Lin, S., Mascarenhas, J.B., Oliveri, F., Xia, J., Casanova, E., Costa, C.F., Brink, M., et al. (2008). Skeletal muscle-specific ablation of raptor, but not of rictor, causes metabolic changes and results in muscle dystrophy. Cell Metab. *8*, 411–424.

Bernardi, R., Guernah, I., Jin, D., Grisendi, S., Alimonti, A., Teruya-Feldstein, J., Cordon-Cardo, C., Simon, M.C., Rafii, S., and Pandolfi, P.P. (2006). PML inhibits HIF-1alpha translation and neoangiogenesis through repression of mTOR. Nature *442*, 779–785.

Csibi, A., Cornille, K., Leibovitch, M.P., Poupon, A., Tintignac, L.A., Sanchez, A.M., and Leibovitch, S.A. (2010). The translation regulatory subunit eIF3f controls the kinase-dependent mTOR signaling required for muscle differentiation and hypertrophy in mouse. PLoS ONE *5*, e8994. 10.1371/journal.pone.0008994.

Cunningham, J.T., Rodgers, J.T., Arlow, D.H., Vazquez, F., Mootha, V.K., and Puigserver, P. (2007). mTOR controls mitochondrial oxidative function through a YY1-PGC-1alpha transcriptional complex. Nature *450*, 736–740.

DeYoung, M.P., Horak, P., Sofer, A., Sgroi, D., and Ellisen, L.W. (2008). Hypoxia regulates TSC1/2-mTOR signaling and tumor suppression through REDD1-mediated 14-3-3 shuttling. Genes Dev. *22*, 239–251.

Evans, R.M. (2005). The nuclear receptor superfamily: a rosetta stone for physiology. Mol. Endocrinol. *19*, 1429–1438.

Fisch, S., Gray, S., Heymans, S., Haldar, S.M., Wang, B., Pfister, O., Cui, L., Kumar, A., Lin, Z., Sen-Banerjee, S., et al. (2007). Kruppel-like factor 15 is a regulator of cardiomyocyte hypertrophy. Proc. Natl. Acad. Sci. USA *104*, 7074–7079.

Gilson, H., Schakman, O., Combaret, L., Lause, P., Grobet, L., Attaix, D., Ketelslegers, J.M., and Thissen, J.P. (2007). Myostatin gene deletion prevents glucocorticoid-induced muscle atrophy. Endocrinology *148*, 452–460.

Glass, D.J. (2003). Signalling pathways that mediate skeletal muscle hypertrophy and atrophy. Nat. Cell Biol. *5*, 87–90.

Gray, S., Wang, B., Orihuela, Y., Hong, E.G., Fisch, S., Haldar, S., Cline, G.W., Kim, J.K., Peroni, O.D., Kahn, B.B., and Jain, M.K. (2007). Regulation of gluconeogenesis by Krüppel-like factor 15. Cell Metab. *5*, 305–312.

Gu, L., Gao, J., Li, Q., Zhu, Y.P., Jia, C.S., Fu, R.Y., Chen, Y., Liao, Q.K., and Ma, Z. (2008). Rapamycin reverses NPM-ALK-induced glucocorticoid resistance in lymphoid tumor cells by inhibiting mTOR signaling pathway, enhancing G1 cell cycle arrest and apoptosis. Leukemia *22*, 2091–2096.

Hoffman, E.P., and Nader, G.A. (2004). Balancing muscle hypertrophy and atrophy. Nat. Med. *10*, 584–585.

Hu, Z., Wang, H., Lee, I.H., Du, J., and Mitch, W.E. (2009). Endogenous glucocorticoids and impaired insulin signaling are both required to stimulate muscle wasting under pathophysiological conditions in mice. J. Clin. Invest. *119*, 3059–3069.

Hundal, H.S., Babij, P., Taylor, P.M., Watt, P.W., and Rennie, M.J. (1991). Effects of corticosteroid on the transport and metabolism of glutamine in rat skeletal muscle. Biochim. Biophys. Acta *1092*, 376–383.

Izumiya, Y., Hopkins, T., Morris, C., Sato, K., Zeng, L., Viereck, J., Hamilton, J.A., Ouchi, N., LeBrasseur, N.K., and Walsh, K. (2008). Fast/Glycolytic muscle fiber growth reduces fat mass and improves metabolic parameters in obese mice. Cell Metab. *7*, 159–172.

Ma, K., Mallidis, C., Artaza, J., Taylor, W., Gonzalez-Cadavid, N., and Bhasin, S. (2001). Characterization of 5′-regulatory region of human myostatin gene: regulation by dexamethasone in vitro. Am. J. Physiol. Endocrinol. Metab. *281*, E1128–E1136.

Mammucari, C., Milan, G., Romanello, V., Masiero, E., Rudolf, R., Del Piccolo, P., Burden, S.J., Di Lisi, R., Sandri, C., Zhao, J., et al. (2007). FoxO3 controls autophagy in skeletal muscle in vivo. Cell Metab. *6*, 458–471.

Matthews, S.E. (1999). Proteins and amino acids. In Modern Nutrition and Health and Diseases, 9th ed., M.E. Shils, J.A. Olson, M. Shike, and A.C. Ross, eds. (Baltimore: Williams & Wilkins), pp. 11–48.

Meijsing, S.H., Pufall, M.A., So, A.Y., Bates, D.L., Chen, L., and Yamamoto, K.R. (2009). DNA binding site sequence directs glucocorticoid receptor structure and activity. Science *324*, 407–410.

Menconi, M., Fareed, M., O'Neal, P., Poylin, V., Wei, W., and Hasselgren, P.O. (2007). Role of glucocorticoids in the molecular regulation of muscle wasting. Crit. Care Med. *35*, S602–S608.

Mizushima, N., Levine, B., Cuervo, A.M., and Klionsky, D.J. (2008). Autophagy fights disease through cellular self-digestion. Nature *451*, 1069–1075.

Moresi, V., Williams, A.H., Meadows, E., Flynn, J.M., Potthoff, M.J., McAnally, J., Shelton, J.M., Backs, J., Klein, W.H., Richardson, J.A., et al. (2010). Myogenin and class II HDACs control neurogenic muscle atrophy by inducing E3 ubiquitin ligases. Cell *143*, 35–45.

Munck, A., Guyre, P.M., and Holbrook, N.J. (1984). Physiological functions of glucocorticoids in stress and their relation to pharmacological actions. Endocr. Rev. *5*, 25–44.

Newgard, C.B., An, J., Bain, J.R., Muehlbauer, M.J., Stevens, R.D., Lien, L.F., Haqq, A.M., Shah, S.H., Arlotto, M., Slentz, C.A., et al. (2009). A branched-chain amino acid-related metabolic signature that differentiates obese and lean humans and contributes to insulin resistance. Cell Metab. *9*, 311–326.

Ning, Y.M., and Sanchez, E.R. (1993). Potentiation of glucocorticoid receptor-mediated gene expression by the immunophilin ligands FK506 and rapamycin. J. Biol. Chem. *268*, 6073–6076.

Risson, V., Mazelin, L., Roceri, M., Sanchez, H., Moncollin, V., Corneloup, C., Richard-Bulteau, H., Vignaud, A., Baas, D., Defour, A., et al. (2009). Muscle inactivation of mTOR causes metabolic and dystrophin defects leading to severe myopathy. J. Cell Biol. *187*, 859–874.

Sancak, Y., Bar-Peled, L., Zoncu, R., Markhard, A.L., Nada, S., and Sabatini, D.M. (2010). Ragulator-Rag complex targets mTORC1 to the lysosomal surface and is necessary for its activation by amino acids. Cell *141*, 290–303.

Sandri, M. (2008). Signaling in muscle atrophy and hypertrophy. Physiology (Bethesda) *23*, 160–170.

Sandri, M., Sandri, C., Gilbert, A., Skurk, C., Calabria, E., Picard, A., Walsh, K., Schiaffino, S., Lecker, S.H., and Goldberg, A.L. (2004). Foxo transcription factors induce the atrophy-related ubiquitin ligase atrogin-1 and cause skeletal muscle atrophy. Cell *117*, 399–412.

Schakman, O., Gilson, H., and Thissen, J.P. (2008). Mechanisms of glucocorticoid-induced myopathy. J. Endocrinol. *197*, 1–10.

Sengupta, S., Peterson, T.R., and Sabatini, D.M. (2010). Regulation of the mTOR complex 1 pathway by nutrients, growth factors, and stress. Mol. Cell *40*, 310–322.

She, P., Reid, T.M., Bronson, S.K., Vary, T.C., Hajnal, A., Lynch, C.J., and Hutson, S.M. (2007). Disruption of BCATm in mice leads to increased energy expenditure associated with the activation of a futile protein turnover cycle. Cell Metab. *6*, 181–194.

Stitt, T.N., Drujan, D., Clarke, B.A., Panaro, F., Timofeyva, Y., Kline, W.O., Gonzalez, M., Yancopoulos, G.D., and Glass, D.J. (2004). The IGF-1/PI3K/Akt pathway prevents expression of muscle atrophy-induced ubiquitin ligases by inhibiting FOXO transcription factors. Mol. Cell *14*, 395–403.

Suzuki, N., Motohashi, N., Uezumi, A., Fukada, S., Yoshimura, T., Itoyama, Y., Aoki, M., Miyagoe-Suzuki, Y., and Takeda, S. (2007). NO production results in suspension-induced muscle atrophy through dislocation of neuronal NOS. J. Clin. Invest. *117*, 2468–2476.

Um, S.H., D'Alessio, D., and Thomas, G. (2006). Nutrient overload, insulin resistance, and ribosomal protein S6 kinase 1, S6K1. Cell Metab. *3*, 393–402.

Waddell, D.S., Baehr, L.M., van den Brandt, J., Johnsen, S.A., Reichardt, H.M., Furlow, J.D., and Bodine, S.C. (2008). The glucocorticoid receptor and FOXO1 synergistically activate the skeletal muscle atrophy-associated MuRF1 gene. Am. J. Physiol. Endocrinol. Metab. *295*, E785–E797.

Wagenmakers, A.J. (1998). Protein and amino acid metabolism in human muscle. Adv. Exp. Med. Biol. *441*, 307–319.

Wang, H., Kubica, N., Ellisen, L.W., Jefferson, L.S., and Kimball, S.R. (2006). Dexamethasone represses signaling through the mammalian target of rapamycin in muscle cells by enhancing expression of REDD1. J. Biol. Chem. *281*, 39128–39134.

Yan, H., Frost, P., Shi, Y., Hoang, B., Sharma, S., Fisher, M., Gera, J., and Lichtenstein, A. (2006a). Mechanism by which mammalian target of rapamycin inhibitors sensitize multiple myeloma cells to dexamethasone-induced apoptosis. Cancer Res. *66*, 2305–2313.

Yoshikawa, N., Nagasaki, M., Sano, M., Tokudome, S., Ueno, K., Shimizu, N., Imoto, S., Miyano, S., Suematsu, M., Fukuda, K., et al. (2009). Ligand-based gene expression profiling reveals novel roles of glucocorticoid receptor in cardiac metabolism. Am. J. Physiol. Endocrinol. Metab. *296*, E1363–E1373.

Yu, L., McPhee, C.K., Zheng, L., Mardones, G.A., Rong, Y., Peng, J., Mi, N., Zhao, Y., Liu, Z., Wan, F., et al. (2010). Termination of autophagy and reformation of lysosomes regulated by mTOR. Nature *465*, 942–946.

Zhao, J., Brault, J.J., Schild, A., Cao, P., Sandri, M., Schiaffino, S., Lecker, S.H., and Goldberg, A.L. (2007). FoxO3 coordinately activates protein degradation by the autophagic/lysosomal and proteasomal pathways in atrophying muscle cells. Cell Metab. *6*, 472–483.

The Status of Exon Skipping as a Therapeutic Approach to Duchenne Muscular Dystrophy

Qi-Long Lu[1], Toshifumi Yokota[2], Shin'ichi Takeda[3], Luis Garcia[4], Francesco Muntoni[5] and Terence Partridge[2]

[1]McColl-Lockwood Laboratory for Muscular Dystrophy Research, Neuromuscular/ALS Center, Carolinas Medical Center, Charlotte, North Carolina, USA; [2]Research Center for Genetic Medicine, Children's National Medical Center, Washington, District of Columbia, USA; [3]Department of Molecular Therapy, National Institute of Neuroscience, National Center of Neurology and Psychiatry, Tokyo, Japan; [4]INSERM U974, UMR 7215 CNRS, Institut de Myologie, UM 76 Université Pierre et Marie Curie, Paris, France; [5]Institute of Child Health, London, UK

Duchenne muscular dystrophy (DMD) is associated with mutations in the dystrophin gene that disrupt the open reading frame whereas the milder Becker's form is associated with mutations which leave an in-frame mRNA transcript that can be translated into a protein that includes the N- and C- terminal functional domains. It has been shown that by excluding specific exons at, or adjacent to, frame-shifting mutations, open reading frame can be restored to an out-of-frame mRNA, leading to the production of a partially functional Becker-like dystrophin protein. Such targeted exclusion can be achieved by administration of oligonucleotides that are complementary to sequences that are crucial to normal splicing of the exon into the transcript. This principle has been validated in mouse and canine models of DMD with a number of variants of oligonucleotide analogue chemistries and by transduction with adeno-associated virus (AAV)-small nuclear RNA (snRNA) reagents encoding the antisense sequence. Two different oligonucleotide agents are now being investigated in human trials for splicing out of exon 51 with some early indications of success at the biochemical level.

Received 23 April 2010; accepted 14 September 2010; published online 26 October 2010. doi:10.1038/mt.2010.219

INTRODUCTION

From the moment of its identification, the Duchenne muscular dystrophy (*DMD*) gene, was clearly going to test the ingenuity of would-be gene therapists. The need to achieve body-wide distribution of the largest known gene is compounded by its structural role as the keystone of a transmembrane cell–surface protein complex; removing the possibility, even with a fully functional protein, of the amplifying effect of an enzyme and implying the need for near-normal molar concentrations to approach normal function. Strange then, that one of the more promising strategies for treating DMD, the skipping of mutated sites, is actually facilitated by the large size and modular structure of dystrophin: its major functional binding sites being separated by a long stretch of rod-like "spacer" that carries no essential function and is the site of the more common DMD mutations.

Use of antisense oligonucleotides to modulate splicing of the dystrophin gene so as to restore a translatable mRNA transcript was mooted some years ago on the basis of *in vitro* data[1,2] but firm evidence for practical utility of this approach awaited studies in the *mdx* mouse model of DMD.[3–6] These, in turn, set in train a concerted effort to advance the technology toward human trials, as summarized in the following accounts of work presented and discussed at a meeting held in the Banbury Center at Cold Spring Harbor from the 14th to the 17th of October 2008.

CHEMISTRY AND MODIFICATIONS: CRUCIAL FOR REALIZING THERAPEUTIC POTENTIAL

Progressive advances in exon skipping for DMD have been related to the application of new antisense oligomer chemistries and their modification for improved delivery (**Figure 1**). The most widely used chemistry is the 2′O-methylphosphorothioate-modified (2′OMePS) antisense oligoribonucleotide (AON). This modification provides resistance to nuclease degradation while retaining negative charge to facilitate effective delivery in cell culture systems by most delivery reagents.[7] The potential of this chemistry for treating DMD was initially demonstrated in dystrophic *mdx* mice[5,6] and more recently by intramuscular injection in DMD patients.[8] However, for systemic delivery, 2′OMePS showed limited efficiency in the *mdx* mouse. Three intravenous (i.v.) injections of 2 mg 2′OMePS/mouse (~60–80 mg/kg) at weekly intervals did induce detectable dystrophin expression in all skeletal muscles, but only in sparse focal patches of muscle fibers within each muscle and never at >5% of normal levels. Disappointingly too, little or no dystrophin expression was seen in cardiac muscle. No toxicity to liver or kidney was observed. Thus, assuming that the preclinical model recapitulates precisely the efficiency and pharmacokinetics of administration to DMD boys, 2′OMePS appear safe but it is uncertain whether their systemic use would induce sufficient dystrophin expression to have a therapeutic impact in DMD boys.[4]

Correspondence: Terence Partridge, Research Center for Genetic Medicine, Children's National Medical Center, 111 Michigan Ave NW, Washington, District of Columbia, USA. E-mail: tpartridge@cnmcresearch.org

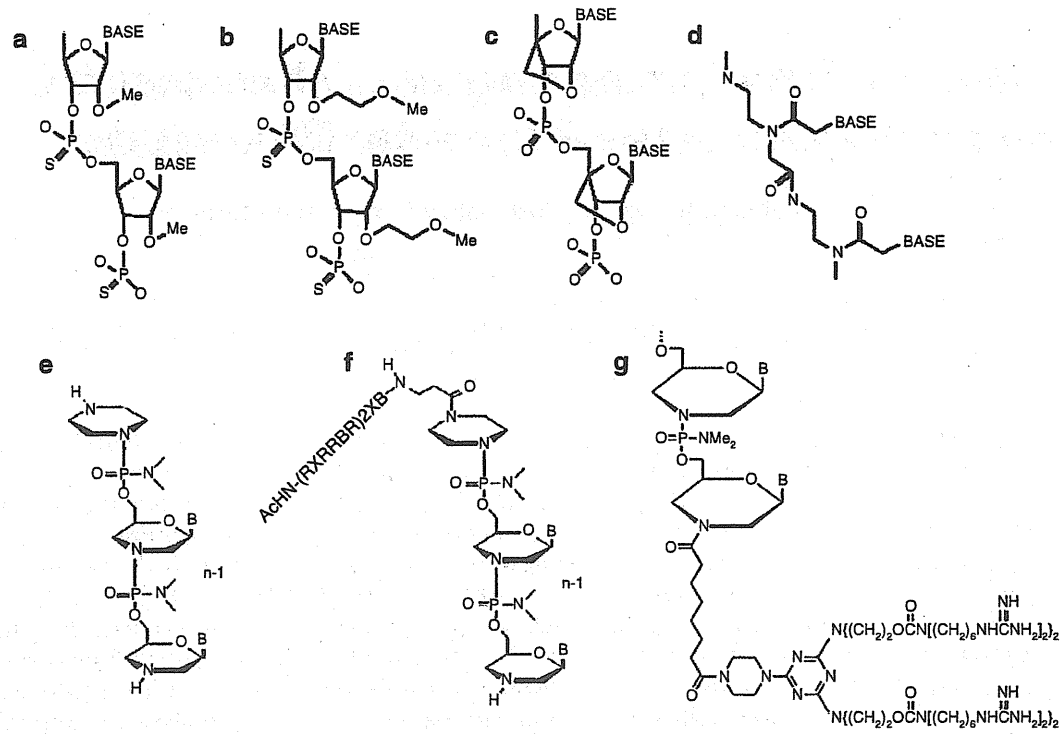

Figure 1 Chemistries of antisense oligomers. (**a**) 2′-O-Methylphosphorothioate (2′OMePS AON); (**b**) 2′-O-methoxyethyl phosphorothioate; (**c**) locked nucleic acid (LNA); (**d**) peptide nucleic acid (PNA); (**e**) phosphorodiamidate morpholino oligomers (PMO); (**f**) AcHN-(RXRRBR)2XB peptide-tagged PMO (R, arginine, X, 6-aminohexanoic acid and B, ®- alanine) (PPMO); G, octa-guanidine PMO.

More recently, phosphorodiamidate morpholino oligomers (PMO) have been explored for exon skipping in the dystrophin gene. In PMO, the phosphodiester bond is replaced by phosphorodiamidate linkage and the ribose replaced by a morpholino moiety (Figure 1). PMOs are charge-neutral and refractory to biological degradation. This chemistry has long been used for translational blockade in zebrafish; penetrating the cells of the developing fishes relatively easily.[9] It has also been applied to cultured mammalian cells[10] where its delivery appears to be impeded by its nonionic nature. In response to this problem, "scrape-loading" (creating pores in the membrane) and "leashing" (complexing PMO with negatively charged complementary DNA sequences) were then developed to enhance delivery by use of commercially available delivery reagents, such as polyethyleneimine and lipofectin.[11] However, on direct injection into muscles the leash adjunct proved toxic and was therefore not tested by i.v. administration. Despite the poor entry of unmodified PMO into cells in tissue culture, it was later found to enter muscle fibers better than 2′OMePS *in vivo* in the dystrophic *mdx* mouse. A single intramuscular injection of 10 μg PMO induced significantly higher levels of dystrophin expression than the same PMO complexed with leash and lipofectin.[3] Furthermore, regular weekly i.v. injections of PMO targeting mouse dystrophin exon 23 induced up to 50% of normal levels of dystrophin in body-wide skeletal muscles in the *mdx* mice, with improved muscle pathology, decreased serum levels of muscle creatine kinase and partial restoration of normalized muscle strength. Even after systemic administration for 1 year, no toxicity has been detected in muscles or other organs. A more recent investigation at higher dosages[12] confirmed that PMO produced higher levels of exon 23 skipping than 2′OMePS and thus appears to be a promising antisense oligomer chemistry for the treatment of DMD patients.[3]

Although both 2′OMePS and PMO induce exon skipping systemically, it was disappointing to find that dystrophin expression was highly variable within and between muscles, even after repeated i.v. injections.[3,4,12] Why this is so, is not clearly understood, but may be due to the reliance on passive diffusion for entry into muscle fibers. For PMO, the lack of charge may present less of an impediment to cell surface contact thus allowing more efficient entry than 2′OMePS into muscle fibers, particularly those with leaky membranes as seen in dystrophic muscles. Such dependence on muscle damage for effective delivery of AONs, would have the advantage of limiting the amount of AON entering untargeted and undamaged nonmuscle cells, thus diminishing possible side effects. However, for long-term effective treatment of DMD, it would carry the disadvantage that muscle fibers rescued by PMO-induced exon skipping would have to re-enter a myopathic state to permit further PMO entry. Such a requirement for recurring cycles of rescue and degeneration in treated muscles could severely limit the value of antisense therapy for DMD patients.

The requirement of muscle damage for effective delivery and AON induced dystrophin expression is further demonstrated by the relative lack of dystophin expression in cardiac muscle of *mdx* mice after systemic injection of either 2′OMePS AON or PMO.[3,4,12] Cardiac muscles in the mice are less affected than skeletal muscle by the dystrophic process and neither conspicuous pathological change nor functional impairment are seen until late stages. Consistently, only trace amounts of dystrophin are detected in